Journal of Constructional Steel Research 151 (2018) 41–57

Contents lists available at ScienceDirect

Journal of Constructional Steel Research

Evaluation of seismic response factors for BRBFs using FEMA P695 methodology

Yasin Onuralp Özkılıç [a], Mehmet Bakır Bozkurt [b], Cem Topkaya [c,*]

[a] Department of Civil Engineering, Necmettin Erbakan University, Konya 42060, Turkey
[b] Department of Civil Engineering, Manisa Celal Bayar University, Manisa 45140, Turkey
[c] Department of Civil Engineering, Middle East Technical University, Ankara 06531, Turkey

ARTICLE INFO

Article history:
Received 12 April 2018
Received in revised form 23 July 2018
Accepted 14 September 2018
Available online xxxx

Keywords:
Buckling-restrained brace
Structural frames
Steel
Seismic
Response factor
Yielding

ABSTRACT

This paper reports the details of a numerical study undertaken to evaluate seismic response factors for steel buckling-restrained braced frames (BRBFs) using the FEMA P695 methodology. In the United States, BRBFs are designed according to Minimum Design Loads for Buildings and Other Structures (ASCE 7) and the Seismic Provisions for Structural Steel Buildings (AISC 341). Twenty-four archetypes were designed according to the U.S. specifications and their behavior was assessed by making use of non-simulated collapse models. The interstory drift, brace axial strain and cumulative brace axial strain demands under collapse level ground motions were determined. The results obtained indicate that the current seismic response factors are adequate in terms of interstory drift and cumulative axial strain demands. On the other hand, large differences between the design level and collapse level axial strains were reported, which can result in undesirable brace behavior. Modified approaches were developed to estimate the axial strains for collapse level ground motions. These include a modification to the deflection amplification factor and a modification to the AISC 341 requirements for expected brace deformations. The archetypes were redesigned using the proposed modifications and reevaluated using the FEMA P695 methodology. The results indicate that the proposed modifications result in axial strain demands that are in close agreement with the calculated demands.

1. Introduction

Steel buckling-restrained braced frames (BRBFs) are often used as lateral load resisting systems against forces produced by wind and earthquakes. BRBFs employ buckling-restrained braces (BRBs) which may be considered as hysteretic dampers. During a seismic event, BRBs yield in tension and compression and contribute to energy dissipation. As shown in Fig. 1, a typical BRB is composed of a core segment, de-bonding material and a buckling restraining mechanism [1,2]. The cross section of the core segment is usually reduced along the length to constrain yielding to a limited domain. The length of the yielding segment can be adjusted to meet the stiffness requirements.

The axial load resistance and axial strain capacity of BRBs are the two most important parameters that should be determined at the design stage. BRB manufacturers use these key parameters to develop designs that meet these objectives. The AISC Seismic Provisions for Structural Steel Buildings (AISC 341) [3] provide guidance on the expected BRB deformation demands. According to this specification, BRBs shall be designed, tested and detailed to accommodate deformations corresponding to a story drift of at least 2% of the story height or two times the design story drift, whichever is larger. Qualifying cyclic tests for BRBs also employ the expected deformation demand as the main parameter for the loading protocol. In addition, individual brace test specimens are required to achieve a cumulative inelastic axial deformation of at least 200 times the yield deformation.

The equivalent lateral force procedure can be used together with a set of seismic response factors to obtain the design story drift. This procedure enables elastic analysis and design which is based on reduced seismic forces. The idea here is that the magnitude of lateral forces is reduced by taking into account the yielding and ductility of the lateral load resisting system. The general structural response shown in Fig. 2 should be considered to view the development of response factors. Their formulation according to Uang [4] is as follows:

$$\mu_s = \frac{\Delta_{\max}}{\Delta_y} \quad R_\mu = \frac{V_e}{V_y} \quad \Omega_o = \frac{V_y}{V_s} \quad R = \frac{V_e}{V_s} = R_\mu \Omega_o \quad C_d = \frac{\Delta_{\max}}{\Delta_s} = \mu_s \Omega_o \tag{1}$$

where, V_e is the ultimate elastic base shear, V_s is the base shear at the first significant yield, V_y is the base shear at the structural collapse level, Δ_s is the drift at the first significant yield, Δ_y is the drift at the structural collapse level, Δ_{max} is the maximum amount of drift, μ_s is the ductility factor, Ω_o is the overstrength factor, R_μ is the ductility reduction

* Corresponding author.
E-mail address: ctopkaya@metu.edu.tr (C. Topkaya).

https://doi.org/10.1016/j.jcsr.2018.09.015
0143-974X/

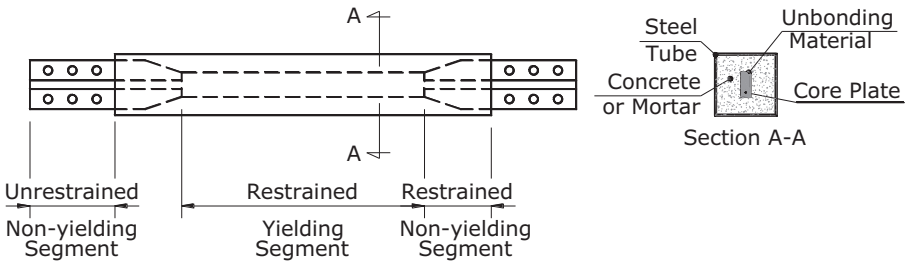

Fig. 1. A typical buckling-restrained brace.

factor, R is the response modification coefficient, and C_d is the deflection amplification factor.

Seismic response factors have been developed for various lateral load resisting systems based on observations from past earthquakes and engineering judgment. These factors vary from one specification to the other. In the United States, seismic response factors for BRBFs are given in Minimum Design Loads for Buildings and Other Structures (ASCE 7) [5]. The recommended values of the response modification coefficient (R), the over-strength factor (Ω_o), and the deflection amplification factor (C_d) are 8, 2.5, and 5, respectively. Brace deformation demands must be reasonably estimated at the design stage for the satisfactory performance of BRBFs. The design and detailing of BRBs are directly influenced by the design axial force and the story drift, which depend on the seismic response factors.

Numerical studies conducted on BRBFs have concentrated on quantifying and reducing the amount of residual drifts [6,7], the effect of different beam-to-column connections [8] and the use of short cores [9]. A few studies were also undertaken to address the issue of response factors. One of the early studies was conducted by Sabelli et al. [10] to explore the inelastic dynamic behavior of BRBFs and to compare it with the behavior of concentrically braced frames. Five stacked chevron (Inverted V) type BRBF archetypes were designed and investigated using nonlinear time history analyses. The primary variables investigated were the response modification coefficient, the flexibility of beams and the level of seismic hazard. Three and 6 story archetypes were designed considering response modification coefficients of 6 and 8. For the 6 story archetypes, stiff and flexible beam cases were studied to examine the effect of beam flexibility on the overall response. Seismic hazard levels corresponding to a 50%, 10%, and 2% probability of exceedance in a 50-year period were considered. The frames were designed on the basis of the equivalent lateral force (ELF) procedure and the designs

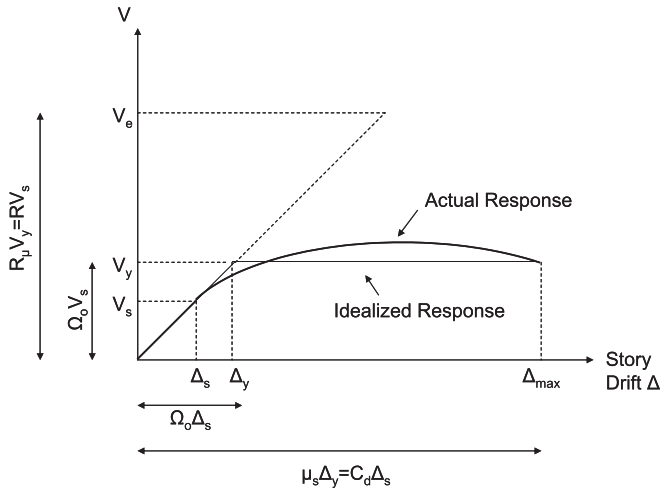

Fig. 2. General structural response.

were governed by the strength of the members, where code displacement criteria were not the controlling factor. The yield strength of the braces was 248 MPa and the yielding segment of the brace had a length of 70% of the total brace length. Columns were modeled as a having fixed bases and all beam-to-column connections with gusset plates attached were modeled as being rigid. The analysis results revealed that the response of the frames is not sensitive to the response modification coefficient selected in the rage of 6 and 8. Stiffening the beam to limit the vertical displacements was found to have only a small effect on the peak lateral displacements. The overall response was found to be influenced significantly by the seismic hazard level. The displaced shape of the frames resembles flexural behavior for the 50% probability events, where larger interstory drifts occur at the top rather than at the bottom. The pattern of deformations was found to change significantly as the severity of earthquakes is increased. For the 10% and especially the 2% percent probability events, drift concentrations in the lower stories were reported. The mean of the maximum drifts under the suite of ground motions considered was reported alongside the maximum elastic drift under design loads. The ratio of the maximum drift to elastic drift is an indication of the displacement amplification factor for BRBF systems. This ratio was observed to vary between 5.7 and 7.8 for the 10% probability events. For the case of a 6 story archetype under the 2% probability events, a ratio of 18.4 was reported which shows a significant increase in displacement demands as the seismic hazard level increases. The highest cumulative brace ductility demands were observed in one of the 6-story archetypes subjected to excitations with a 2% probability of exceedance in 50 years. The mean and mean plus one standard deviation cases resulted in brace ductility demands of 139 and 185 times the yield deformation respectively.

Fahnestock et al. [11] conducted a numerical study on the seismic response and performance of BRBFs. The study compiled results from the numerical studies of Sabelli et al. [10], Iwata et al. [12] and Mayes et al. [13]. In addition, the performance of a chevron-type 4-story BRBF archetype was studied under the Design Basis Earthquake (DBE) and the Maximum Considered Earthquake (MCE). The BRBF archetype was designed using $R = 8$ and $C_d = 5.5$, which were the values recommended by ASCE 7 at that time. The first story columns were connected to the columns at the basement level and this ensured a substantially rigid column base at the first story. A bolted beam splice connection was modeled for the regions where the beams are attached to columns. The study revealed that the performance of the BRBF archetype was acceptable and met the Life Safety performance criterion under DBE and the Near Collapse criterion under MCE. The value of the deflection amplification factor (C_d) was shown to provide unconservative estimates of the inelastic lateral displacements and a C_d factor of 8 was recommended for BRBFs. In addition, the method for predicting BRB maximum brace ductility demands, which also depend on the C_d factor, was found to provide unconservative estimates. A more rigorous method was developed that takes into account various adjustment factors.

A methodology was developed by FEMA to quantify the building seismic response (performance) factors (FEMA P695) [14]. This methodology offers a systematic way of determining the response factors

for new structural systems and can also be used for existing systems. Beta testing of the methodology was conducted on different lateral load resisting systems including BRBFs [15]. The BRBF study employed 10 archetypes with two story X-brace configuration and a number of stories varying between 2 and 16. Two seismic hazard levels were considered and the systems were designed with either ELF procedure or response spectrum analysis (RSA). The methodology recommends using $C_d = R$ for new systems and this strategy was employed in the evaluation process. In other words, the archetypes were designed based on the response factors recommended by ASCE 7, except that the C_d value was considered to be equal to 8.0. The beam-to-column connections were considered to be rigid, and the column bases were modeled as fixed. The collapse simulations included various aspects of behavior, including P-Δ effects and the low cycle fatigue behavior of BRBs, where each brace was assumed to have a cumulative inelastic deformation capacity of 200 times the yield deformation. The maximum amount of brace axial strain was not included as a performance parameter. The results revealed that all of the 10 archetypes satisfied the performance objectives and showed that the recommended values of response factors are acceptable, provided that $C_d = R$ is utilized.

Recently, Speicher and Harris [16] evaluated six BRBF archetypes using four analysis procedures given in ASCE 41 [17]. Several recommendations were developed based on the evaluation of the results. The authors concluded that the BRBF building probability of collapse (given MCE) should be determined via a FEMA P695 analysis to benchmark the performance relative to the design intent of ASCE 7.

Past numerical studies on BRBF response factors point to various deficiencies especially in the selection of the displacement amplification factor (C_d). Most of the studies reported to date concentrated on a limited number of BRBF archetypes where the variations in the type of BRBF, material strength, design constraints, BRB yielding length, and column base conditions are not systematically evaluated. In this paper, 24 archetypes are designed using the response factors currently recommended by ASCE 7 and evaluated using the methodology outlined in FEMA P695 to provide an in-depth assessment of BRBF performance. The results are presented by concentrating on the interstory drifts, brace axial strains, and cumulative brace axial strains and by comparing the values obtained at the design stage with the ones obtained from non-linear time history analysis. A complementary study is undertaken to examine the deflection amplification factor. The results of this study are used to propose a deflection amplification factor that varies over the height of the structure. Furthermore, the differences in deformation demands between DBE and collapse level ground motions are explored. A modification to AISC 341 requirements for expected brace deformations is proposed. The proposed modifications are applied to the 24 archetypes and their improvements are demonstrated.

2. Overview of the FEMA P695 methodology

The FEMA Methodology requires nonlinear collapse simulation on the selected archetype models. Collapse simulation is conducted using a far-field record set that consists of 22 pairs of ground motions. All 44 ground motion records must be individually applied to an archetype in cases where a two dimensional analysis is performed. The ground motion records are scaled twice. The first scaling is required to anchor the median spectrum of the far-field record set to the MCE response spectra at the fundamental period of the archetype. The second scaling is applied successively to all far-field ground motions until 50% of the archetypes exhibit collapse. The amount of scaling that results in the collapse of 50% of the archetypes is compared with a variable named the Adjusted Collapse Margin Ratio (*ACMR*). The target *ACMR* values are tabulated in the FEMA P695 document and depend on the total system collapse uncertainty (β_{TOT}), and collapse probability. Two conditions must be satisfied for acceptable performance. The average value of *ACMR* for each performance group should meet the target *ACMR* for 10% collapse probability ($ACMR_{10\%}$). Furthermore, the *ACMR* value for each index archetype within a performance group should meet the target *ACMR* for 20% collapse probability ($ACMR_{20\%}$). While a successive scaling approach can be adopted for new structural systems, the scaling of all ground motions using a pre-calculated scaling factor is sufficient for the evaluation of existing systems. In the present study, individual archetypes, rather than performance groups, were considered. The 10% probability of collapse was adopted as a criterion for *ACMR* (i.e. $ACMR_{10\%}$) according to Appendix F4.2 of FEMA P695 which applies to collapse evaluation of individual buildings. The total system collapse uncertainty (β_{TOT}) depends on various factors, such as, record-to-record collapse uncertainty, design requirements-related collapse uncertainty, test data-related collapse uncertainty, and modeling-related collapse uncertainty.

3. Design and selection of archetypes

Different Seismic Design Categories (SDC) may be adopted in the Methodology in order to represent the variations in seismic hazard. In the present study, only one seismic design category, namely, SDC D_{max} was considered, which represents the highest seismic hazard level. Beta testing of the Methodology [15] on BRBFs showed that the response modification coefficient is governed by the highest seismic hazard level, while the overstrength factor is governed by other seismic hazard levels such as D_{min}. According to FEMA P695, the MCE, 5% damped, spectral response acceleration parameter at short periods adjusted after site class effects (S_{MS}) was considered as 1.50 g, for D_{max}. Similarly, the MCE, 5% damped, spectral response acceleration parameter at a period of 1 s adjusted after site class effects (S_{M1}) was taken as 0.90 g.

Two geometrical configurations have been adopted for BRBFs where the first one employs single diagonal braces, and the second one employs chevron type braces. Each configuration can also be subdivided into categories. The single diagonal braces may be in the form of zigzag bracing (ZZ bracing) or lightening bolt bracing (LB bracing) whereas the chevron type braces may be single story chevron type or 2-story X-braces [15]. Both the LB type single diagonal and single story chevron type configurations were considered.

Only one type of floor plan, shown in Fig. 3, was considered. This floor plan was originally used by Lopez and Sabelli [18] to exemplify BRBF design. The floor plan is rectangular with side dimensions of 36 m and 22.8 m. There are four bays with single diagonal BRBFs in the long direction of the floor plan which are indicated as BF-1 in Fig. 3. Two bays with chevron type BRBFs are employed in the short direction of the floor plan which are indicated as BF-2 in Fig. 3. Both the BF-1 and BF-2 type frames were designed as a part of this study. All beam-to-column connections and the column bases of the BRBF were considered simple connections with no moment transfer, so as to study the most critical case where the contribution from moment frame action is eliminated. A dead load of 5 kN/m^2 and a live load of 2 kN/m^2 which are typical for steel office buildings were considered as the loading. The story height was taken as 3.5 m for all stories except the first story where the height was equal to 4.3 m. In order to take into account variations in structural periods, 3, 6, and 9 story BRBFs were considered. Typical elevation plans for single diagonal and chevron type 9-story BRBFs are shown in Fig. 4.

Variations in the mechanical and geometrical properties of the BRB core plate were taken into account. Two common types of steel grades were considered. The core plates of BRBs were designed using A992 grade steel with a yield strength of 345 MPa, which is a common type of structural steel used in the U.S. In addition, these plates were designed using S235 grade steel with a yield strength of 235 MPa, which is a common type of structural steel used in Europe. Previous studies by Sabelli et al. [10] and Fahnestock et al. [11] considered yield strengths of 248 MPa and 317 MPa respectively. The length of the yielding segment of a BRB depends on the BRB type and the required stiffness of the brace. In the present study, two different yielding lengths were

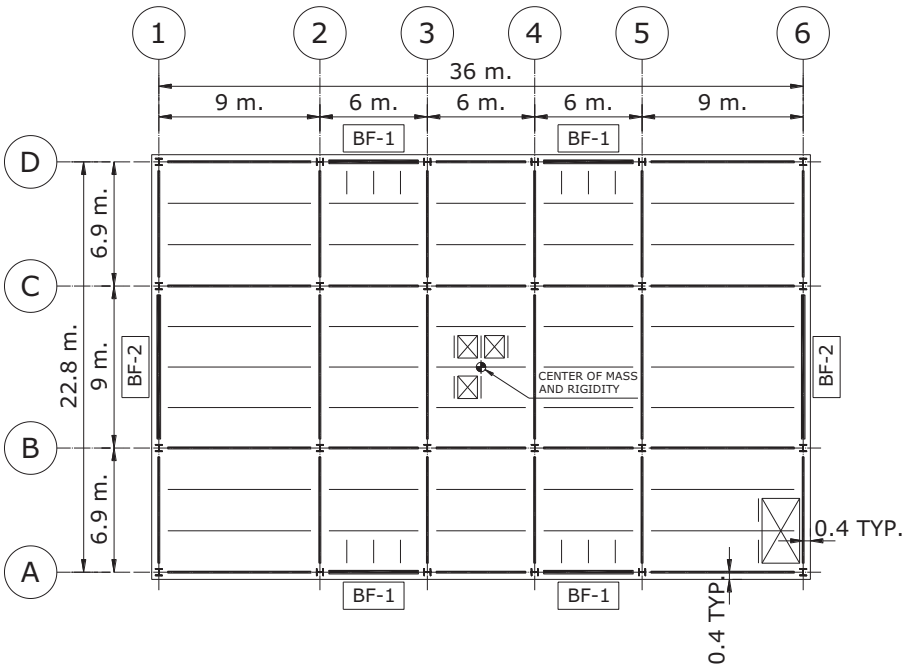

Fig. 3. Floor plan used in the study.

considered where the length of the yielding segment is either 1/2 or 2/3 of the total length of the BRB. These proportions are typical for the BRBs available in the market. The distance between the workpoints of beam-column-brace intersections at each end of the brace was used to determine the total length of a BRB. The non-yielding segments of BRBs were assumed to have an area equal to twice the area of the yielding segment. A992 grade steel was assumed for all other members of the seismic load resisting system.

The combinations of different numbers of stories, type of bracing, yield strength of BRB core and the length of the yielding segment resulted in 24 archetypes to be designed. Designs were carried out according to ASCE 7 [5], AISC 341 [3], and AISC 360 [19]. The ELF procedure was used and the archetypes were designed by minimizing the weight of the framing. Capacity design principles were used in design of beam and column members. The design steps followed the procedure explained by Lopez and Sabelli [18], including adjustment factors. A generic backbone curve presented by Lopez and Sabelli [18] was used for determining the tension and compression strength adjustment factors depending on the level of expected brace ductility. A W16 × 50 section was used for the beams in all stories of the archetypes. Columns and BRB core plate sizes are given in Tables 1 and 2 for the chevron and single diagonal archetypes respectively. It should be noted that the selected column sizes do not differ for BRBs with different plate dimensions. The design of chevron type BRBFs is governed by the strength limit states. Owing to their large bay width, the interstory drift limitation of 2% was satisfied for the combination of beam, column and brace sizes, determined

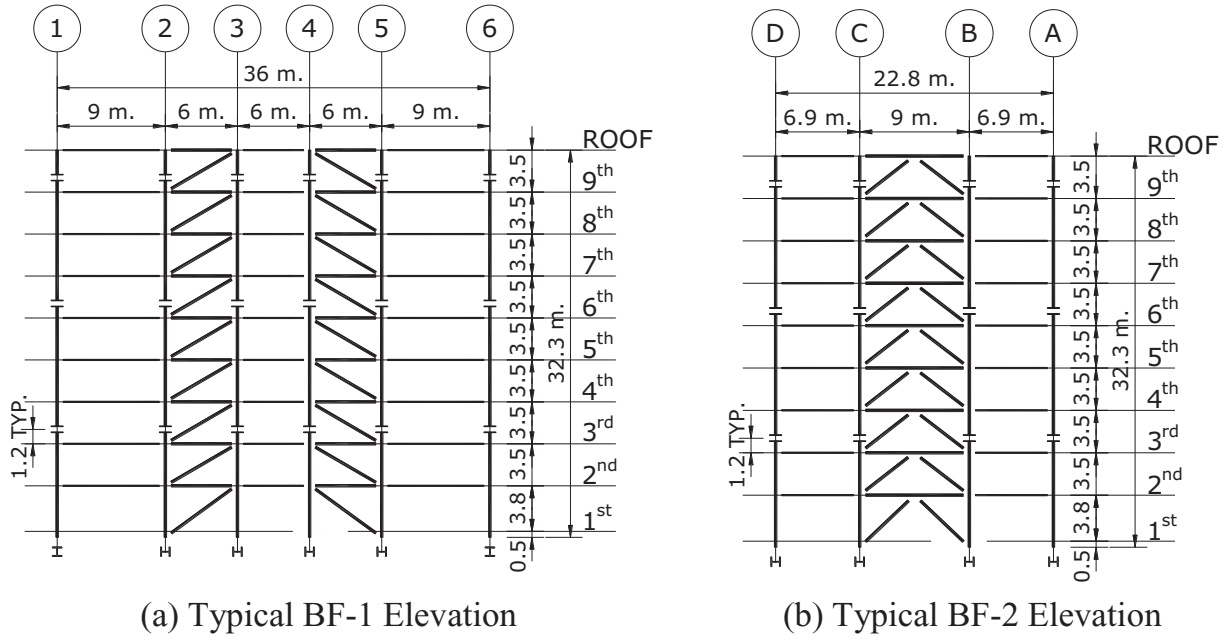

Fig. 4. Typical elevation plans for 9-story BRBFs.

Table 1
Column and brace sizes of Chevron archetypes.

NS	S	Columns	Braces (Original and Redesigned)				
			A992–2/3	A992–1/2	S235–2/3	S235–1/2	S235–1/2 - RSA
3	1	W14 × 68	15 × 146	15 × 146	15 × 214	15 × 214	–
	2	W14 × 68	15 × 123	15 × 123	15 × 180	15 × 180	–
	3	W14 × 38	15 × 90.5	15 × 90.5	15 × 133	15 × 133	–
6	1	W14 × 132	25 × 113	25 × 113	25 × 163	25 × 163	–
	2	W14 × 132	25 × 97	25 × 97	25 × 142	25 × 142	–
	3	W14 × 68	25 × 89	25 × 89	25 × 131	25 × 131	–
	4	W14 × 68	25 × 79	25 × 79	25 × 116	25 × 116	–
	5	W14 × 48	25 × 65	25 × 65	25 × 95	25 × 95	–
	6	W14 × 48	25 × 47	25 × 47	25 × 69	25 × 69	–
9	1	W14 × 132	25 × 112	25 × 112	25 × 164	25 × 164	25 × 164
	2	W14 × 132	25 × 104	25 × 104	25 × 153	25 × 153	25 × 148
	3	W14 × 132	25 × 103	25 × 103	25 × 151	25 × 151	25 × 137
	4	W14 × 132	25 × 98	25 × 98	25 × 144	25 × 144	25 × 126
	5	W14 × 68	25 × 92	25 × 92	25 × 135	25 × 135	25 × 116
	6	W14 × 68	25 × 84	25 × 84	25 × 123	25 × 123	25 × 109
	7	W14 × 53	25 × 73	25 × 73	25 × 107	25 × 107	25 × 100
	8	W14 × 53	25 × 59.5	25 × 59.5	25 × 87	25 × 87	25 × 90
	9	W14 × 53	25 × 43	25 × 43	25 × 63	25 × 63	25 × 70

NS: Number of Stories; S: Story Number, RSA: Response Spectrum Analysis.

based on strength limit states. While the same observation is true for 3-story single diagonal BRBFs, drift limits were the controlling factor for the 6- and 9-story single diagonal BRBFs. The brace core areas had to be increased to meet the interstory drift limits for these frames.

The key design parameters for all of the archetypes are reported in Tables 3 through 6. In these tables the design interstory drift ratios and the design axial strains for the BRB members are given. The design axial strains were calculated according to the requirements of AISC 341, where the expected deformations are calculated based on story drift of at least 2% of the story height or two times the design story drift, whichever is larger. A rigid plastic mechanism similar to the one proposed by Tremblay et al. [20] was employed to estimate the brace axial strains from the design story drift. In this mechanism, the beam and columns of a story are assumed to be rigid, and the brace is the only member that deforms. The following equation provides a geometrical relationship between the elastic interstory drift angle θ_s (interstory drift divided by the story height) and the anticipated brace axial strain

$$\varepsilon_{br} = 2 \times \frac{C_d \times \theta_s}{\alpha} \times \sin\theta \times \cos\theta \quad (2)$$

where θ is the brace angle measured with respect to a horizontal axis, α is the ratio of the yielding length of a BRB to its total length. The above formulation is conservative in a sense because it neglects the axial shortening and elongation effects of the columns. The static structural analysis of a BRBF, which is used to determine θ_s, takes into account the axial deformation of the columns. For the nonlinear range of behavior, the effects of column shortening and elongations can be included by conducting a nonlinear pushover analysis, or by hand calculations similar to the one given by Bosco et al. [21].

In this paper the axial strain demands and cumulative demands are calculated for the yielding segment of BRBs. This is in contrast to considering the total BRB axial deformation which includes the deformations of the non-yielding segments. The two measures provide similar demands as the area of the non-yielding segment becomes very large in comparison to the area of the yielding segment.

4. Numerical modeling of archetypes and application of the methodology

The performances of the designed archetypes were evaluated by making use of numerical analysis. The OPENSEES [22] computational framework was used for numerical simulations. Two-dimensional finite element models were used to model the archetypes. The beams and columns of the archetypes were modeled with nonlinear beam-column elements. The yielding parts of the BRBs were modeled with nonlinear truss elements, whereas the non-yielding parts were modeled using nonlinear beam-column elements. In general, one of the BRBF bays was modeled and the tributary mass was added to two of the nodes at every story. Leaning columns carrying gravity loads were linked to the frame to simulate P-Δ effects. Pin connections were modeled at the ends of the beams to prevent any kind of moment transfer from the beams to the columns or braces. Similarly the column bases were also modeled as pinned bases. The hysteretic behavior of BRBs was simulated using the steel02 material model which is to be found in the OPENSEES library. The coefficients for this model were taken as $b = 0.02$, $R0 = 20$, $R1 = 0.925$, and $R2 = 0.15$ based on the test results from Bozkurt and Topkaya [23] in order to match the strength level at 2% axial deformation. According to the adopted material model the BRB axial resistance increases by 30% due to strain hardening when it experiences an axial strain of 2%. Zona and Dall'Asta [24] demonstrated the significant role of isotropic hardening in modeling BRB behavior. The steel02 material model is based on the Giuffre-Menegotto-Pinto steel material with isotropic strain hardening. A comparison of the experimental response for Specimen 7, which has been reported by

Table 2
Column and brace sizes of single diagonal archetypes.

NS	S	Columns	Braces (Original)				Braces (Redesigned)			
			A992–2/3	A992–1/2	S235–2/3	S235–1/2	A992–2/3	A992–1/2	S235–2/3	S235–1/2
3	1	W14 × 48	15 × 95.5	15 × 95.5	15 × 142	15 × 142	15 × 155	15 × 125	15 × 155	15 × 142
	2	W14 × 48	15 × 75	15 × 75	15 × 110	15 × 110	15 × 120	15 × 97	15 × 120	15 × 110
	3	W14 × 38	15 × 44.5	15 × 44.5	15 × 65.5	15 × 65.5	15 × 72	15 × 58	15 × 72	15 × 65.5
6	1	W14 × 68	25 × 95	25 × 83	25 × 105	25 × 105	25 × 140	25 × 124	25 × 140	25 × 124
	2	W14 × 68	25 × 85	25 × 75	25 × 94	25 × 94	25 × 124	25 × 111	25 × 124	25 × 111
	3	W14 × 53	25 × 77	25 × 67	25 × 86	25 × 86	25 × 113	25 × 101	25 × 113	25 × 101
	4	W14 × 53	25 × 66	25 × 58	25 × 73	25 × 73	25 × 96	25 × 86	25 × 96	25 × 86
	5	W14 × 38	25 × 49	25 × 44	25 × 54.5	25 × 54.5	25 × 72	25 × 64	25 × 72	25 × 64
	6	W14 × 38	25 × 27	25 × 24	25 × 30.5	25 × 30.5	25 × 40	25 × 35.5	25 × 40	25 × 35.5
9	1	W14 × 132	25 × 132	25 × 115	25 × 132	25 × 119	25 × 151	25 × 136	25 × 151	25 × 136
	2	W14 × 132	25 × 119	25 × 104	25 × 119	25 × 107	25 × 136	25 × 122	25 × 136	25 × 122
	3	W14 × 132	25 × 116	25 × 102	25 × 116	25 × 105	25 × 133	25 × 119	25 × 133	25 × 119
	4	W14 × 132	25 × 110	25 × 97	25 × 110	25 × 99	25 × 125	25 × 113	25 × 125	25 × 113
	5	W14 × 68	25 × 101	25 × 88	25 × 101	25 × 91	25 × 115	25 × 103	25 × 115	25 × 103
	6	W14 × 68	25 × 88	25 × 78	25 × 88	25 × 79.5	25 × 101	25 × 91	25 × 101	25 × 91
	7	W14 × 53	25 × 72	25 × 64	25 × 72	25 × 65	25 × 82	25 × 74	25 × 82	25 × 74
	8	W14 × 53	25 × 52	25 × 46	25 × 52	25 × 47	25 × 60.5	25 × 55	25 × 60.5	25 × 55
	9	W14 × 53	25 × 28.5	25 × 25	25 × 28	25 × 25.5	25 × 34.5	25 × 31	25 × 34.5	25 × 31

NS: Number of Stories; S: Story Number.

Table 3
Percent interstory drift ratios for Chevron archetypes.

		A992–2/3			A992–1/2			S235–2/3			S235–1/2		
		Design		Ana.	Design		Ana.	Design		Ana.	Design		Ana.
NS	S	O	R		O	R		O	R		O	R	
3	1	1.10	1.76	3.90	1.01	1.61	4.63	0.80	1.27	4.29	0.73	1.17	4.52
	2	1.05	1.47	3.06	0.96	1.34	3.57	0.77	1.07	3.35	0.71	0.99	3.68
	3	0.81	0.97	1.47	0.74	0.89	2.10	0.58	0.69	1.54	0.53	0.63	2.01
6	1	1.10	1.76	5.02	1.01	1.62	4.60	0.82	1.31	4.63	0.76	1.22	4.73
	2	1.23	1.72	4.61	1.13	1.59	4.29	0.93	1.30	4.25	0.86	1.20	4.26
	3	1.28	1.54	3.52	1.19	1.43	3.47	0.97	1.16	3.25	0.91	1.09	3.37
	4	1.30	1.30	2.39	1.21	1.21	2.36	1.01	1.01	2.09	0.95	0.95	2.24
	5	1.27	1.27	1.58	1.19	1.19	1.61	1.01	1.01	1.33	0.96	0.96	1.47
	6	1.12	1.12	1.28	0.90	0.90	1.19	0.91	0.91	0.93	0.71	0.71	0.87
9	1	1.23	1.97	5.37	1.13	1.81	4.62	0.90	1.45	4.59	0.84	1.34	4.09
	2	1.41	1.98	4.43	1.32	1.84	3.79	1.09	1.52	3.77	1.02	1.43	3.56
	3	1.53	1.84	3.49	1.44	1.72	3.03	1.21	1.46	2.93	1.15	1.37	2.94
	4	1.63	1.63	2.93	1.53	1.53	2.56	1.31	1.31	2.38	1.24	1.24	2.42
	5	1.68	1.68	1.94	1.58	1.58	1.99	1.37	1.37	1.66	1.30	1.30	1.84
	6	1.73	1.73	1.47	1.64	1.64	1.48	1.43	1.43	1.29	1.37	1.37	1.26
	7	1.73	1.73	1.23	1.64	1.64	1.21	1.45	1.45	1.13	1.39	1.39	1.10
	8	1.64	1.64	1.20	1.56	1.56	1.16	1.39	1.39	1.10	1.34	1.34	1.04
	9	1.39	1.39	1.06	1.33	1.33	0.99	1.19	1.19	0.82	1.15	1.15	0.75

NS: Number of Stories; S: Story Number, O: Original Design; R: Revised Design; Ana.: Analysis Result.

Bozkurt and Topkaya [23], and the numerical response is given in Fig. 5. While isotropic hardening is taken into account, the adopted material model does not simulate the higher compressive resistance of a BRB when compared with its tensile resistance.

The total system collapse uncertainty is dependent on four factors, three of which require judgment. These factors depend on the knowledge level and modeling capabilities related to the system of interest. BRBFs have been studied for over 15 years and have been implemented in practice. In addition, computational models for BRBFs were also developed and the simulation of BRBF behavior can be achieved with confidence. Therefore, high quality level ((A) Superior) was assigned to design requirements-related collapse uncertainty ($\beta_{DR} = 0.1$), test data-related collapse uncertainty ($\beta_{TD} = 0.1$), and modeling-related collapse uncertainty ($\beta_{MDL} = 0.1$). The fourth factor that needs to be considered is the record-to-record collapse uncertainty (β_{RTR}) which depends on the period-based ductility (μ_T). The μ_T values were determined by conducting a nonlinear static (pushover) analysis in accordance with ASCE 41 and are reported in Table 7. The following expressions which are given in FEMA P695 were used to calculate β_{RTR} and β_{TOT}.

$$\beta_{RTR} = 0.1 + 0.1 \times \mu_T \leq 0.4 \tag{3}$$

$$\beta_{TOT} = \sqrt{\beta^2{}_{RTR} + \beta^2{}_{DR} + \beta^2{}_{TD} + \beta^2{}_{MDL}} \tag{4}$$

The $ACMR_{10\%}$ values were determined according to Table 7-3 of FEMA P695, by using the total system collapse uncertainty (β_{TOT}). Normally the record set needs to be scaled until 50% of the records cause the collapse of an archetype. The methodology was modified to a certain extent in the present study. The archetypes were subjected to collapse level ground motions by considering the target $ACMR_{10\%}$ value. The scaling to be applied to the ground motion set was determined by considering two scaling factors SF_1, and SF_2, which are reported in Table 7. The response spectra for the 44 ground motions are presented in Fig. 6. According to the methodology the records have to be scaled first by a

Table 4
Percent brace axial strains and ductility demands for Chevron archetypes.

		A992–2/3				A992–1/2				S235–2/3				S235–1/2			
		Design		Analysis		Design		Analysis		Design		Analysis		Design		Analysis	
NS	S	O	R	ST	D	O	R	ST	D	O	R	ST	D	O	R	ST	D
3	1	1.7	4.0	2.8	16	2.0	4.9	4.4	25	1.5	2.9	3.1	27	2.0	3.5	4.4	37
	2	1.5	3.2	2.1	12	1.9	3.9	3.8	22	1.5	2.3	2.3	20	1.9	2.9	3.9	33
	3	1.5	2.2	1.0	6	1.9	2.9	2.2	12	1.5	2.2	1.0	9	1.9	2.9	2.1	17
6	1	1.7	4.0	3.6	21	2.0	4.9	4.3	25	1.5	3.0	3.3	28	2.0	3.6	4.5	38
	2	1.8	3.8	3.2	18	2.2	4.6	4.6	27	1.5	2.8	3.0	25	1.9	3.5	4.5	38
	3	1.9	3.4	2.4	14	2.3	4.2	3.6	21	1.5	2.6	2.2	19	1.9	3.2	3.5	30
	4	1.9	2.8	1.6	9	2.4	3.5	2.4	14	1.5	2.2	1.4	12	1.9	2.9	2.3	19
	5	1.9	2.2	1.0	6	2.3	3.5	1.5	9	1.5	2.2	0.8	7	1.9	2.9	1.4	12
	6	1.6	2.2	0.8	5	1.9	2.9	1.1	6	1.5	2.2	0.6	5	1.9	2.9	0.8	7
9	1	1.9	4.5	4.0	23	2.3	5.4	4.5	26	1.5	3.3	3.4	29	2.0	4.0	3.9	33
	2	2.1	4.3	3.1	18	2.6	5.4	4.0	23	1.6	3.3	2.6	22	2.0	4.2	3.7	32
	3	2.2	4.0	2.4	14	2.8	5.0	3.1	18	1.8	3.2	2.0	17	2.2	4.0	3.0	25
	4	2.4	3.6	1.9	11	3.0	4.5	2.5	15	1.9	2.9	1.6	13	2.4	3.6	2.4	20
	5	2.4	3.7	1.3	7	3.1	4.6	2.0	12	2.0	3.0	1.1	9	2.5	3.8	1.7	14
	6	2.5	3.8	0.9	5	3.2	4.8	1.3	8	2.1	3.1	0.8	7	2.7	4.0	1.1	9
	7	2.5	3.8	0.7	4	3.2	4.8	1.0	6	2.1	3.2	0.6	5	2.7	4.0	0.9	8
	8	2.4	3.6	0.7	4	3.0	4.6	1.0	6	2.0	3.0	0.6	5	2.6	3.9	0.8	7
	9	2.0	3.0	0.6	4	2.6	3.9	0.8	5	1.7	2.6	0.5	4	2.2	3.4	0.5	5

NS: Number of Stories; S: Story Number, O: Original Design; R: Revised Design; ST: Percent Strain; D: Ductility Demand.

Table 5
Percent interstory drift ratios for single diagonal archetypes.

		A992–2/3			A992–1/2			S235–2/3			S235–1/2		
		Design		Ana.	Design		Ana.	Design		Ana.	Design		Ana.
NS	S	O	R		O	R		O	R		O	R	
3	1	1.62	1.74	5.42	1.48	1.90	5.06	1.16	1.74	4.54	1.07	1.56	4.68
	2	1.91	2.00	4.62	1.76	2.00	4.59	1.45	2.00	4.22	1.33	1.84	4.14
	3	1.89	1.67	5.21	1.75	1.70	5.14	1.38	1.67	4.45	1.30	1.53	4.56
6	1	1.37	1.93	4.91	1.41	1.95	4.92	1.28	1.93	5.69	1.18	1.95	4.61
	2	1.78	1.99	5.03	1.81	2.00	4.93	1.67	1.99	5.14	1.57	2.00	4.24
	3	1.93	1.87	3.97	1.97	1.88	3.74	1.81	1.87	3.79	1.71	1.88	3.36
	4	1.97	1.59	2.79	2.00	1.60	2.84	1.87	1.59	2.76	1.76	1.60	2.64
	5	1.99	1.59	2.44	2.00	1.61	2.32	1.87	1.59	2.43	1.78	1.61	2.19
	6	1.94	1.53	2.71	1.96	1.54	2.62	1.81	1.53	2.38	1.72	1.54	2.30
9	1	1.29	1.90	3.68	1.32	1.90	3.82	1.29	1.90	4.45	1.30	1.90	4.42
	2	1.53	1.99	3.26	1.56	1.99	3.40	1.53	1.99	4.05	1.53	1.99	4.14
	3	1.67	1.86	2.97	1.69	1.87	2.87	1.67	1.86	3.53	1.66	1.87	3.59
	4	1.75	1.64	2.46	1.77	1.64	2.56	1.75	1.64	3.07	1.75	1.64	3.18
	5	1.88	1.77	1.96	1.91	1.78	2.19	1.88	1.77	2.29	1.88	1.78	2.34
	6	1.95	1.84	1.85	1.97	1.84	1.90	1.95	1.84	1.72	1.95	1.84	1.86
	7	1.99	1.88	1.99	2.00	1.87	1.84	1.99	1.88	1.58	1.99	1.87	1.64
	8	1.96	1.83	2.46	1.98	1.82	2.15	1.96	1.83	1.87	1.96	1.82	1.73
	9	1.89	1.74	3.09	1.92	1.74	2.65	1.90	1.74	2.24	1.90	1.74	2.06

NS: Number of Stories; S: Story Number, O: Original Design; R: Revised Design; Ana.: Analysis Result.

factor SF_1, which anchors the spectral acceleration of the median of the records to the design spectrum at the fundamental period of the structure. These scale factors are provided in the Appendix of the FEMA P695 document. The fundamental period of vibration is determined by multiplying the lower bound period, determined according to ASCE 7, with the coefficient $C_u = 1.4$. These approximate periods are reported in Table 7, alongside the fundamental periods calculated from eigenvalue analysis. The scaling of the records to anchor to the design spectrum is demonstrated in Fig. 7 for archetype #5, which is a 6 story chevron braced frame with A992 braces and having a yielding length ratio of 1/2. For this archetype, the fundamental period to be used in design was determined as 1.03 s. For this period, the unscaled acceleration spectra has an ordinate of 0.337 g. According to FEMA P695, the ground motion set should be scaled by $SF_1 = 2.57$ to anchor the ordinate to 0.866 g which corresponds to the MCE level seismic input. The methodology defines the Collapse Margin Ratio (*CMR*) as the ratio between the median collapse intensity and the MCE intensity. In order to take into account the frequency content (spectral shape) of the ground motion set, the *CMR* is modified by a Spectral Shape Factor (*SSF*), which depends on the fundamental period and μ_T. The *SSF* value for each archetype is given in Table 7. The second scaling factor (SF_2), which is equal to *CMR*, is determined by using the following relationship

$$SF_2 = CMR = \frac{ACMR_{10\%}}{SSF} \tag{5}$$

For the archetype #5 the *SSF* and $ACMR_{10\%}$ were determined as 1.34 and 1.746 respectively. By using Eq. (5), the *CMR* value which represents the second scaling (SF_2) to be applied is determined as 1.30. As shown in Fig. 7, the record set has be scaled by a factor $SF = SF_1 \times SF_2 = 2.57 \times 1.30 = 3.34$ for collapse level ground motion simulations. This scaling results in a spectral acceleration of 1.126 g at the fundamental period of the structure.

The archetypes were subjected to 44 ground motion records and the records were scaled by the scaling factors (*SF*) listed in Table 7. A 2%

Table 6
Percent brace axial strains and ductility demands for single diagonal archetypes.

		A992–2/3				A992–1/2				S235–2/3				S235–1/2			
		Design		Analysis		Design		Analysis		Design		Analysis		Design		Analysis	
NS	S	O	R	ST	D	O	R	ST	D	O	R	ST	D	O	R	ST	D
3	1	2.3	3.7	3.8	22	2.8	5.4	4.6	27	1.7	3.7	3.2	27	2.0	4.4	4.3	37
	2	2.5	3.9	2.9	17	3.1	5.2	3.8	22	1.9	3.9	2.6	22	2.3	4.8	3.4	29
	3	2.5	3.3	3.3	19	3.0	4.5	4.2	25	1.8	3.3	2.8	24	2.3	4.0	3.8	32
6	1	2.0	4.1	3.4	20	2.7	5.6	4.5	26	1.8	4.1	4.0	34	2.2	5.6	4.2	36
	2	2.3	3.9	3.1	18	3.2	5.2	4.0	23	2.2	3.9	3.2	27	2.7	5.2	3.4	29
	3	2.5	3.7	2.4	14	3.4	4.9	3.1	18	2.4	3.7	2.3	20	3.0	4.9	2.7	23
	4	2.6	3.1	1.6	9	3.5	4.2	2.2	12	2.4	3.1	1.6	14	3.1	4.2	2.1	17
	5	2.6	3.1	1.4	8	3.5	4.2	1.8	10	2.4	3.1	1.4	12	3.1	4.2	1.6	14
	6	2.5	3.0	1.6	9	3.4	4.0	2.0	12	2.4	3.0	1.4	12	3.0	4.0	1.8	15
9	1	1.7	4.1	2.5	15	2.7	5.4	3.5	20	1.9	4.1	3.1	26	2.6	5.4	4.1	35
	2	1.9	3.9	1.9	11	3.0	5.2	2.7	15	2.2	3.9	2.5	21	3.0	5.2	3.4	29
	3	2.1	3.6	1.7	10	3.3	4.9	2.2	13	2.4	3.6	2.1	18	3.2	4.9	2.9	25
	4	2.2	3.2	1.4	8	3.4	4.3	1.9	11	2.5	3.2	1.8	16	3.4	4.3	2.5	21
	5	2.4	3.5	1.1	6	3.7	4.7	1.5	9	2.7	3.5	1.4	12	3.7	4.7	1.7	15
	6	2.5	3.6	0.9	5	3.8	4.8	1.3	7	2.8	3.6	0.9	8	3.8	4.8	1.4	12
	7	2.6	3.7	1.0	6	3.9	4.9	1.2	7	2.9	3.7	0.9	7	3.9	4.9	1.2	10
	8	2.6	3.6	1.4	8	3.8	4.8	1.6	9	2.9	3.6	1.1	9	3.8	4.8	1.3	11
	9	2.6	3.4	1.9	11	3.7	4.6	2.1	12	2.8	3.4	1.3	11	3.7	4.6	1.6	13

NS: Number of Stories; S: Story Number, O: Original Design; R: Revised Design; ST: Percent Strain; D: Ductility Demand.

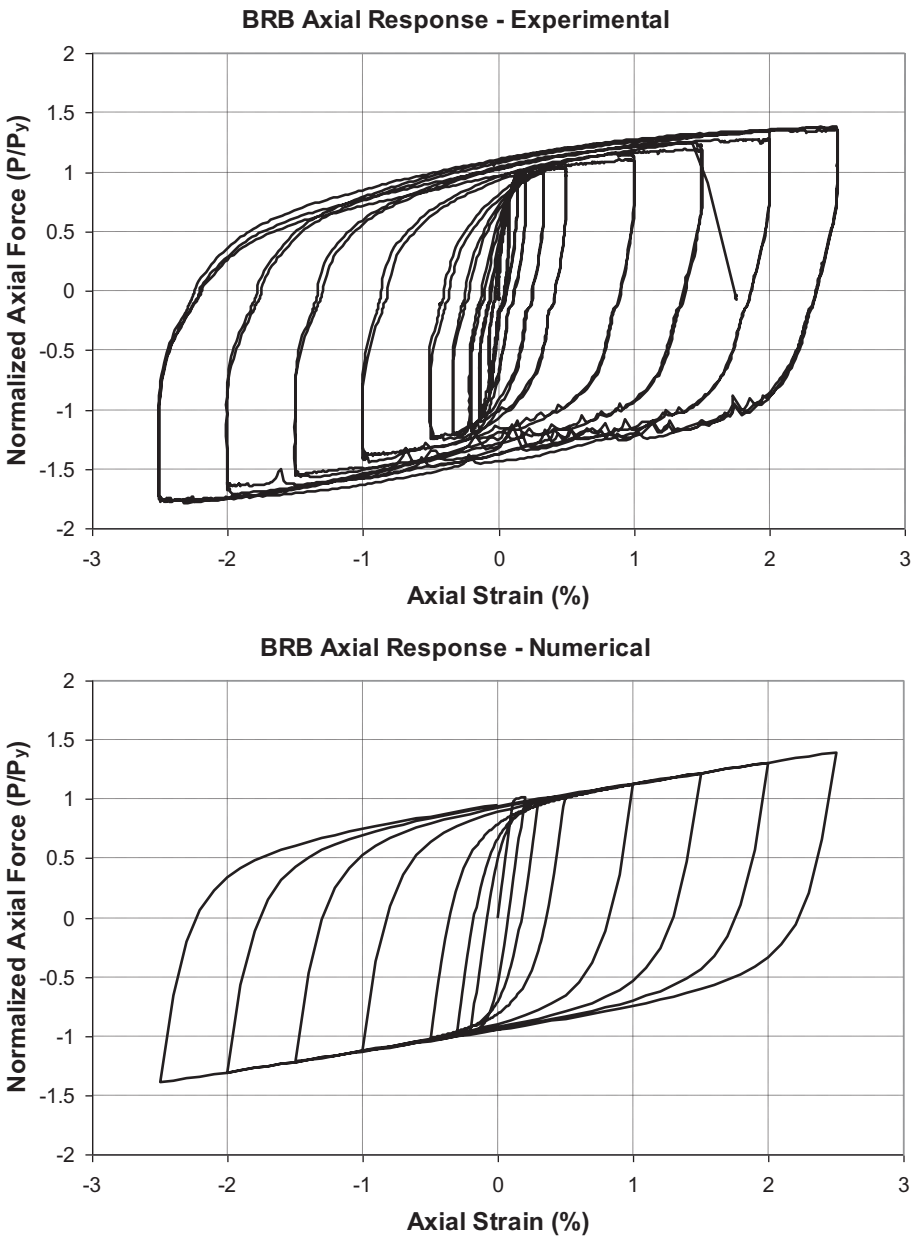

Fig. 5. Comparison of experimental and numerical responses of BRBs.

mass and stiffness proportional damping was used in the time history analysis for all vibration modes.

5. Evaluation of response factors

The methodology enables one to use non-simulated collapse models for collapse failure modes that cannot be modeled explicitly. Non-simulated collapse modes can be indirectly evaluated using alternative limit state checks on structural response quantities measured in the analysis. Buckling-restrained braces generally exhibit stable behavior followed by fracture as shown in Fig. 5. Fracture in steel members is difficult to simulate and the methodology allows for non-simulated collapse models where fracture in members is expected. Brace fracture results in a story-mechanism which can trigger collapse. The response of a frame after brace fracture depends on many factors including, but not limited to, the strength of non-structural elements and the redundancy of the system. Three non-simulated collapse models were considered, namely, the interstory drift ratio, the brace axial strain (ductility demand), and the cumulative axial strain. According to FEMA P695, median values of these response quantities were calculated at the collapse level seismic input and were considered in the evaluation process. The results from the time history analysis are presented separately in the following sections.

5.1. Interstory drift ratio

The median interstory drift ratios under collapse level ground motions are given in Tables 3 and 5. This response parameter was examined in detail to assess whether or not a story type of collapse mechanism occurs. The behavior of beam-columns under axial load and the inelastic rotation demand resulting from story drift is an active research field [25,26]. Experimental studies have shown that the interstory drift capacity of columns depends on many factors such as the axial load level, the local slenderness of the web or flange, and the global slenderness. W14 sections that are typically employed in BRBFs were found to have interstory drift capacities that range between 7%–9% [25] under an

Table 7
Archetype properties and scaling factors.

AN	B	NS	YS	YL	T	TC	SF_1	μ_T	β_{RTR}	β_{TOT}	ACMR	SSF	CMR (SF_2)	SF
1	C	3	345	2/3	0.63	0.75	2.46	5.34	0.400	0.436	1.746	1.29	1.36	3.35
2	C	6	345	2/3	1.03	1.32	2.57	3.89	0.400	0.436	1.746	1.31	1.34	3.44
3	C	9	345	2/3	1.36	2.03	2.51	3.07	0.400	0.436	1.746	1.31	1.33	3.34
4	C	3	345	1/2	0.63	0.71	2.46	5.76	0.400	0.436	1.746	1.30	1.35	3.31
5	C	6	345	1/2	1.03	1.26	2.57	4.39	0.400	0.436	1.746	1.34	1.30	3.34
6	C	9	345	1/2	1.36	1.96	2.51	2.76	0.376	0.414	1.698	1.29	1.32	3.31
7	C	3	235	2/3	0.63	0.64	2.46	6.50	0.400	0.436	1.746	1.32	1.32	3.25
8	C	6	235	2/3	1.03	1.15	2.57	4.52	0.400	0.436	1.746	1.33	1.31	3.37
9	C	9	235	2/3	1.36	1.80	2.51	2.85	0.385	0.422	1.714	1.29	1.32	3.32
10	C	3	235	1/2	0.63	0.61	2.46	4.34	0.400	0.436	1.746	1.25	1.39	3.43
11	C	6	235	1/2	1.03	1.11	2.57	3.26	0.400	0.436	1.746	1.27	1.37	3.54
12	C	9	235	1/2	1.36	1.75	2.51	2.70	0.370	0.409	1.688	1.28	1.32	3.31
13	S	3	345	2/3	0.63	0.99	2.46	7.41	0.400	0.436	1.746	1.35	1.29	3.18
14	S	6	345	2/3	1.03	1.60	2.57	4.27	0.400	0.436	1.746	1.32	1.32	3.40
15	S	9	345	2/3	1.36	2.14	2.51	3.17	0.400	0.436	1.746	1.32	1.32	3.32
16	S	3	345	1/2	0.63	0.95	2.46	6.13	0.400	0.436	1.746	1.31	1.33	3.28
17	S	6	345	1/2	1.03	1.61	2.57	3.96	0.400	0.436	1.746	1.31	1.34	3.44
18	S	9	345	1/2	1.36	2.15	2.51	3.00	0.400	0.436	1.746	1.31	1.34	3.35
19	S	3	235	2/3	0.63	0.85	2.46	7.70	0.400	0.436	1.746	1.35	1.30	3.19
20	S	6	235	2/3	1.03	1.55	2.57	3.06	0.400	0.436	1.746	1.26	1.39	3.57
21	S	9	235	2/3	1.36	2.14	2.51	3.21	0.400	0.436	1.746	1.32	1.32	3.31
22	S	3	235	1/2	0.63	0.82	2.46	6.03	0.400	0.436	1.746	1.31	1.33	3.27
23	S	6	235	1/2	1.03	1.50	2.57	3.98	0.400	0.436	1.746	1.31	1.33	3.43
24	S	9	235	1/2	1.36	2.14	2.51	3.14	0.400	0.436	1.746	1.31	1.33	3.34

AN: archetype number, *B*: type of bracing *C*: chevron, *S*: single diagonal, *NS*: number of story, *YS*: yield strength in MPa, *YL*: yielding length ratio, *T*: fundamental period used in design, *TC*: calculated fundamental period, SF_1: First scaling factor for anchoring far-field record set to MCE spectral demand, μ_T: period-based ductility of an index archetype model, β_{RTR}: record-to-record collapse uncertainty, β_{TOT}: total system collapse uncertainty, *ACMR*: Adjusted collapse margin ratio, *SSF*: Spectral shape factor, *CMR*: Collapse margin ratio, *SF*: Scaling factor.

axial load of 75% of the nominal yield strength. The specimens had slenderness ratios (L_b/r_y) that range between 42.2 and 47.9. W24 sections that are typically employed in moment resisting frame columns were found to have interstory drift capacities that are as low as 1% [26]. These specimens had slenderness ratios that vary between 71 and 161. In the beta testing of the methodology, an interstory drift capacity of 10% was selected for the non-simulated failure criteria of the columns based on the work of Newell and Uang [25]. Fahnestock et al. [11] considered a maximum interstory drift of 4% for the Near Collapse performance level.

The analysis results showed that the maximum interstory drift ratios are 5.37 and 5.69 for the chevron and single diagonal archetypes respectively. In general, most of the median interstory drifts, reported in Tables 3 and 5, stayed below 5%. The experimental study of Newell and Uang [25] demonstrated that the W14 sections used in the columns of the archetypes are capable of resisting the high axial loads under an interstory drift of 5% without any degradation in strength. The results indicate that current response factors provide an adequate margin of safety against collapse when the interstory drift is considered as a criterion.

According to AISC 341, the deformation capacity of a BRB should be determined based on the maximum inelastic drift of a story. When the linear analysis method is employed, the maximum inelastic drift is defined as twice the design story drift. The commentary to AISC 341 states that for nonlinear time history analyses, the maximum inelastic drifts can be taken directly from the analysis results without any need for amplification. The value of two times the design story drift for expected brace deformations represents the mean of the maximum story response for ground motions having a 10% chance of exceedance in 50 years (i.e. the DBE level) [10]. Near-field ground motions, as well as stronger ground motions, can impose deformation demands on braces larger than those required by the AISC 341 provisions.

The interstory drift demands for collapse level earthquakes are compared with the interstory drifts calculated at the design stage. In order to

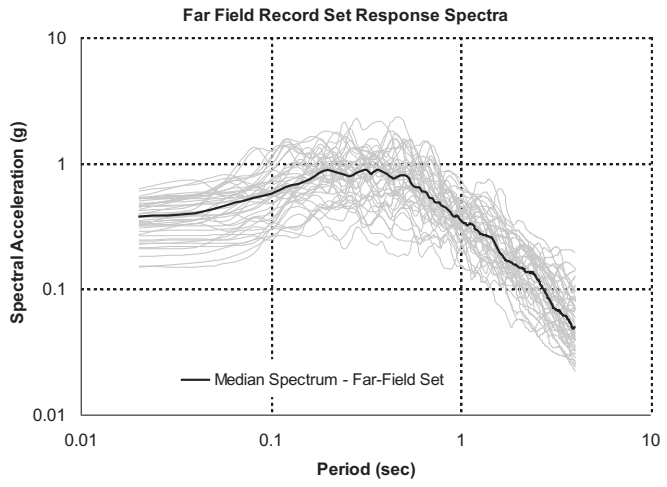

Fig. 6. Far-field record set response spectra.

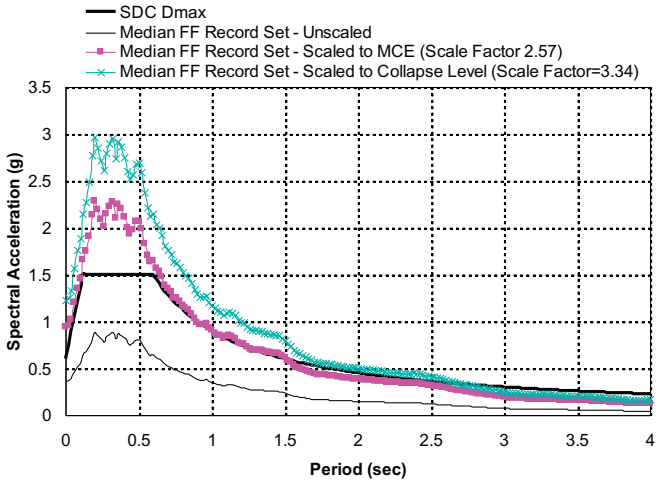

Fig. 7. Scaling of the far-field record set for archetype #5.

make a fair comparison, the median interstory drifts obtained from time history analyses are normalized by two times the design interstory drift and have been depicted in Fig. 8 for all the archetypes. The idea here is to document the level of increase in the interstory drift demands when collapse level ground motions are considered rather than just the DBE level events. Fahnestock et al. [11] recommended two factors namely $C_h = 1.7$ and $C_e = 1.3$ to calculate the maximum brace axial strains from the design interstory drift. C_h is an earthquake hazard level adjustment factor relating the MCE-level response to the DBE-level response. C_e is an evaluation level adjustment factor relating the mean plus standard deviation response to the mean response. The combined effect of C_h and C_e (i.e. $C_h \times C_e$) is an amplification of the design story drift by a factor of 2.21. It should be noted that $C_d = R$ is utilized in the method proposed by Fahnestock et al. [11]. Considering two times the design story drift is equivalent to using $C_d = 2 \times 5 = 10$ in predicting the mean inelastic story drifts for the DBE-level. According to Fig. 8, the ratios of drifts are not constant but rather vary over the height. It is observed that significant amounts of differences are obtained for lower stories where the ratios exceed 3.0. When $C_d = 10$ is considered, the amplification factor of 2.21 recommended by Fahnestock et al. [11] is modified to 1.77 ($2.21 \times R/C_d = 2.21 \times 8/10$). The results given in Fig. 8

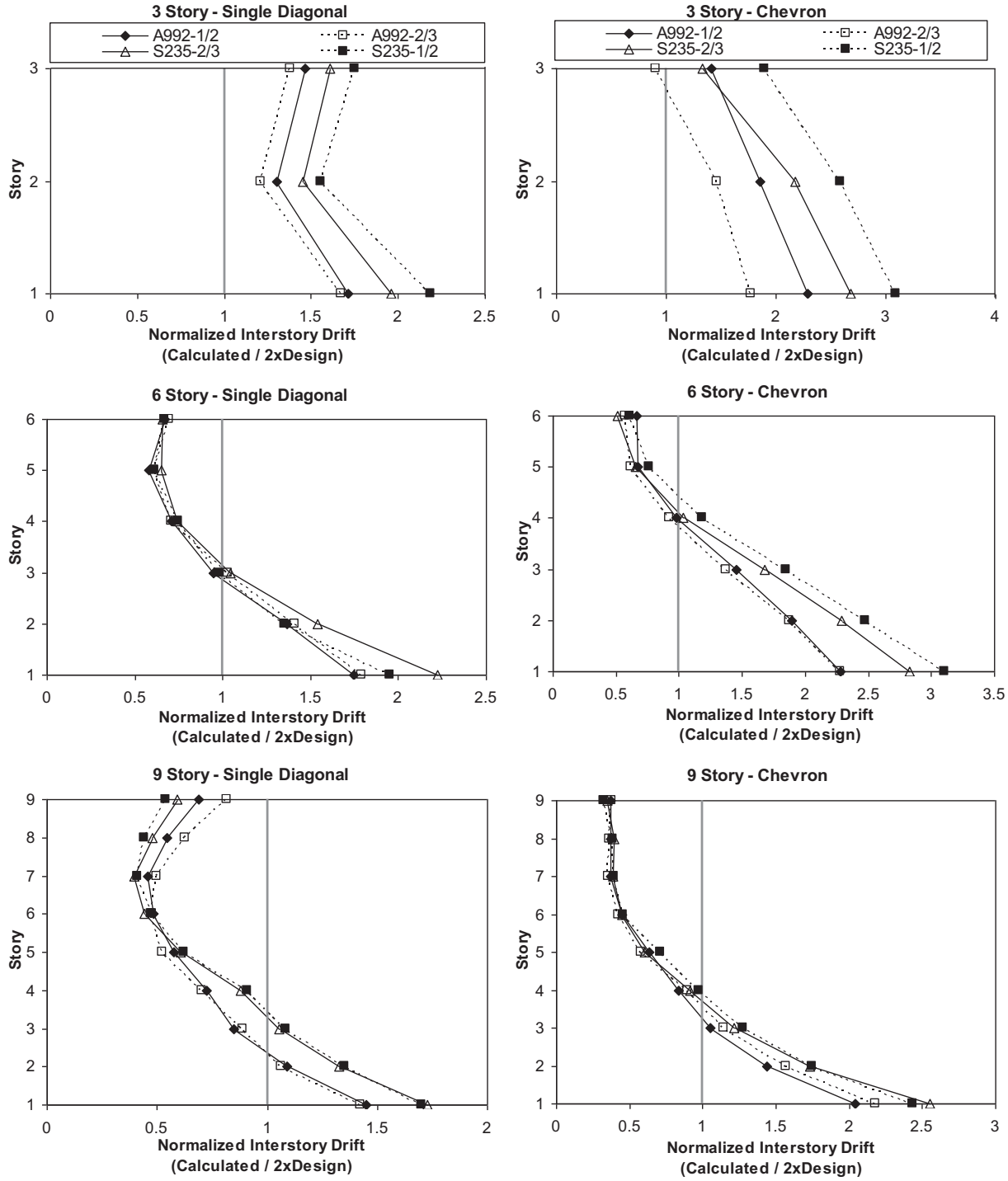

Fig. 8. Normalized interstory drift for all archetypes.

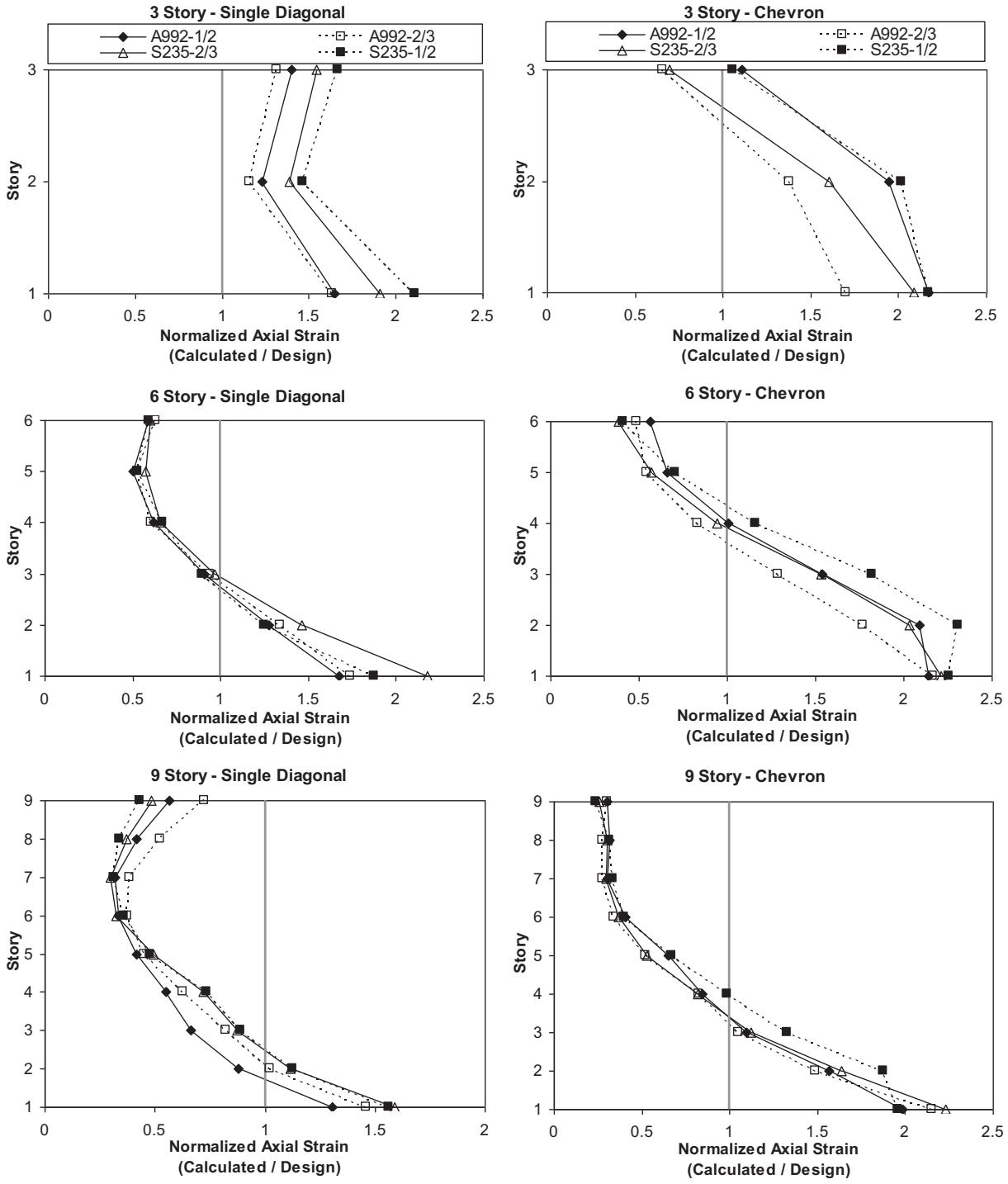

Fig. 9. Normalized brace axial strain for all archetypes.

indicate that the collapse level earthquake produces even higher inelastic interstory drift demands than would be expected for the mean plus standard deviation response obtained at the MCE-level (i.e. comparing 3.0 with 1.77).

5.2. BRB axial strain and ductility demand

The axial strains calculated at the design stage and the median of the axial strains obtained from time history analyses are reported in Tables 4 and 6, for the chevron and single diagonal frames respectively. In these tables the ductility demands in BRBs corresponding to collapse level ground motions are also given. The maximum strain demands vary between 4%–4.6% for most of the archetypes. These strains correspond to an axial deformation ductility of 26 and 38 times the yield deformation for A992 and S235 cores respectively. Fahnestock et al. [11] considered an axial deformation ductility of 25 for the Near Collapse performance level. Both these ductility values exceed the limit considered by Fahnestock et al. [11].

The axial strain (ductility) demand is the most critical parameter in the design of a BRB. The clearance provided between the core and the buckling restraining mechanism directly depends on the strain level to be accommodated. If a lower clearance is provided, the BRB

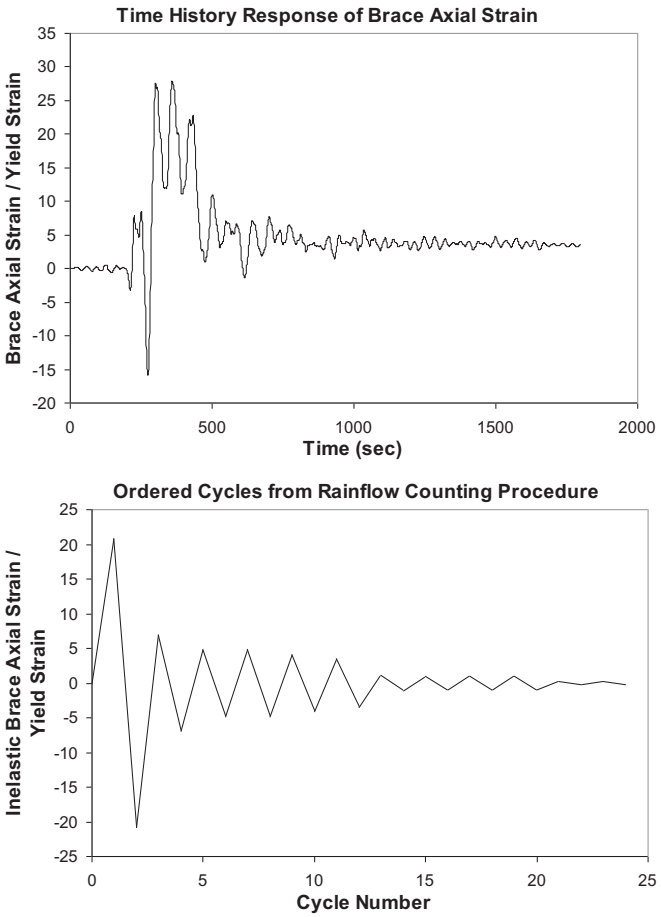

Fig. 10. Rainflow counting to determine cumulative brace axial strain.

core cannot freely move and can come into contact with the buckling restraining mechanism, resulting in the development of excessive axial compressive forces. The unexpected large compression force may cause buckling or connection failure. Furthermore, qualification testing of BRB members is conducted based on the axial strain demand. Most of the BRBs used in practical applications were tested under 2.5% maximum axial strain (ductility ratio of 15) [27]. Recent research papers demonstrate that BRBs with axial strain capacities of the order of 3%–3.5% can be developed [28,29]. The amount of clearance depends on the brace manufacturer. Because the braces are required to be tested under the calculated axial strain demands, providing a larger clearance than would be required is left to the manufacturers' judgment. In cases where the provided clearances are close to the calculated demands, large forces in BRB members can develop under compressive actions. In addition, even if a larger clearance is provided, current designs do not guarantee brace axial strain capacities of the order of 4.5%.

The median axial strains from time history analysis were normalized by the design axial strains and the ratios are shown in Fig. 9. The results indicate that the ratios can exceed 2.0 and can reach up to 2.25. An underestimation of the BRB axial strain demands has a paramount influence on the BRBF performance as explained earlier. The evaluation of BRB axial strains showed a potential weakness in the design process, which is directly attributable to the selection of response factors and to the level of seismic events considered. The low level of axial strain demands is a result of under-estimating the story displacements at the design stage. A potential remedy for this problem is presented in the following sections of the paper.

5.3. BRB cumulative axial strain

While the maximum amount of axial strain is important in order to assess the adequacy of a BRB member, the cumulative axial strains should also be investigated. A brace may experience many cycles of axial strains with lower amplitude and this can result in fracture of the brace due to low cycle fatigue. For this purpose, the axial strain histories under 44 ground motions were extracted from the results of time history analyses. The cumulative amount of axial strain was calculated using the rainflow counting procedure and the cumulative axial strain was expressed in terms of the yield strain. A representative calculation for the cumulative axial strain is given in Fig. 10 for the first story brace of a 9-story chevron archetype with A992 core plates with a yielding length of 1/2 of the total length. In Fig. 10 the axial strain history of this brace under ground motion record CAPEMEND/RIO270 is presented. This record is processed using the rainflow counting procedure to convert the time history response to ordered cycles as shown in Fig. 10. The cumulative axial strain is calculated by summing the amplitudes of the ordered cycles for cycle amplitudes greater than the yield strain. In this particular example the brace member is subjected to a maximum axial strain equal to of 27 times the yield strain. The cumulative strain is calculated as 198 times the yield strain from the ordered cycles.

The medians of cumulative axial strain demands were normalized by the codified demand of 200 and are reported in Fig. 11 for all archetypes. According to this figure, the ratios mostly stayed below unity indicating that no brace fractures are expected under collapse level. The findings are in line with those available from previous studies. Fahnestock et al. [11] and Sabelli et al. [10] reported cumulative axial strains that are 179 and 139 times the yield strains respectively considering mean of the MCE level events. These values modify to 391 and 185 when the mean plus one standard deviation is considered.

The 200 limit was exceeded in some of the archetypes where cumulative strains of the order of 240 to 300 are reported. Most of the experiments conducted on BRBs [27] demonstrated cumulative axial strain capacities greater than 300. Therefore, the response factors provide acceptable designs when complemented with the cumulative axial strain limit of 200.

6. Proposed modifications

Two modifications were developed to estimate the axial strain demand of BRB members under collapse level ground motions. The first of these is a modification of the displacement amplification factor, which would provide more accurate interstory displacement for DBE level response. The second is a modification of the recommendations for the expected deformations of a BRB given in AISC 341. This modification takes into account the differences in demands between the DBE level and collapse level ground motions.

6.1. Modification of the displacement amplification factor

The results presented in the previous section have demonstrated that current values of response factors can result in underestimation of the BRB axial strain demands. This is due to an underestimation of the interstory drifts which are directly influenced by the deflection amplification factor. According to Newmark's equal displacement rule the deflection amplification factor should be equal to the response modification coefficient ($C_d = R$) [30]. Uang and Maarouf [31] demonstrated that C_d values used in the specifications can result in unconservative estimates of lateral displacements. A complementary study was undertaken to study the deflection amplification factor for BRBFs. Pursuant to this goal, four 9-story archetypes were considered. These archetypes were analyzed under DBE level ground motions. For each of the 44 ground motions two separate analyses were conducted. In the first analysis, the frame was modeled to exhibit elastic behavior. In the second

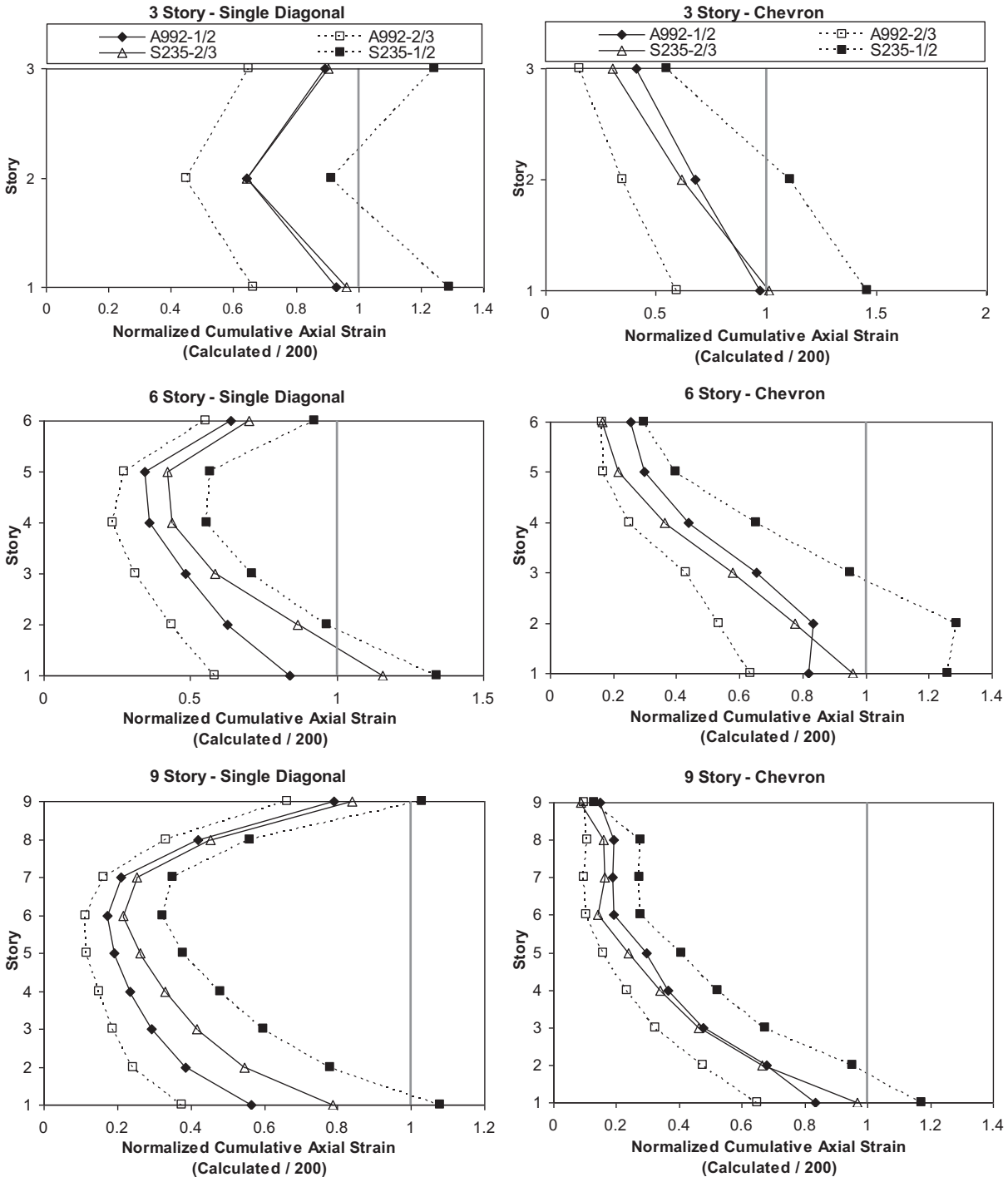

Fig. 11. Normalized cumulative brace axial strain for all archetypes.

analysis, the inelastic behavior of the frame is taken into account. The maximum lateral deflections of the frames at every story were recorded and the median value under the 44 ground motions was calculated.

The analysis results are presented in Fig. 12 in normalized form. The story drift obtained from inelastic time history analysis was normalized by the design story drift and also by the story drift obtained from linear time history analysis. The first of these ratios provides the deflection amplification factor (C_d) whereas the second of these ratios can be used to extend Newmark's equal displacement rule to multi-degree of freedom BRBFs. The analysis results shown in Fig. 12 indicate that the drifts accumulate in the first three stories. The accumulation of drifts was responsible for observing very high brace axial strains, as explored in earlier parts of the paper. In the first story, the C_d value went up to 11 for the chevron type BRBF employing braces with a yield strength of 235 MPa and having a yielding length equal to 1/2 of the total brace length. Furthermore, marked differences were observed between the chevron type and single diagonal type BRBFs. The chevron type bracing system accumulated more drift at the lower stories when compared with the single diagonal bracing system. The ratios of the inelastic drift to elastic drift also show a variation over the height. Normally, the ratios of these drifts are expected to be close to unity according to Newmark's equal displacement rule. However, the analysis results

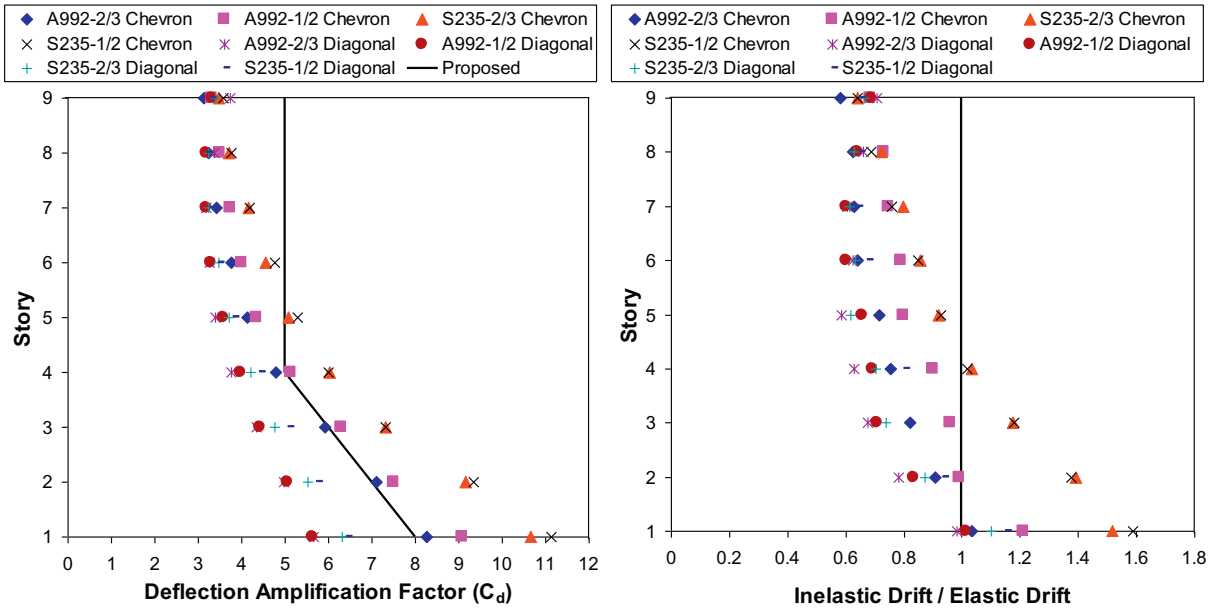

Fig. 12. Proposed Cd factor.

indicate that the inelastic drifts can be more than 60% of the elastic drifts for the lower stories. For the 9th story, the ratios vary between 0.6 and 0.7 depending on the archetype.

The analysis results show that considering a constant value of C_d determined based on the value at the lowest story may lead to over-design of the BRBF systems. The reported C_d values for the 9th story frames vary between 3.11 and 3.73. This indicates that the current value of C_d can be adopted for the upper stories while some corrective measures should be applied to the lower stories. The following C_d profile which is indicated in Fig. 12 was proposed to remedy the problem:

$$C_d = 5\phi_i \quad \text{where} \quad \phi_i = \frac{9-i}{5} \geq 1.0 \tag{6}$$

where i: ith story. The proposed modification was similar in concept to a proposal for deflection amplification factor for eccentrically braced frames [32,33]. According to Eq. (6) the proposed deflection amplification is equal to the response modification coefficient value of 8.0 at the lowest story. The C_d value gradually decreases to 5.0 at the fourth story and stays constant afterwards. Eq. (6) was developed by considering 9 story BRBFs. For taller frames it is recommended to use this equation for the first 9 stories and $C_d = 5$ for stories above the 9th story.

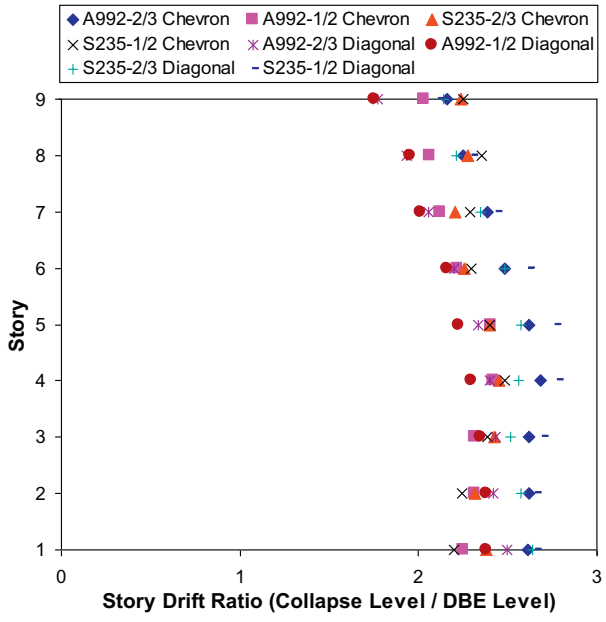

Fig. 13. Ratios of story drifts from collapse level and DBE level ground motions.

6.2. Modification to recommendations of AISC 341

The BRB axial strains can be more accurately determined from interstory drifts by adopting Eq. (6). This evaluation, however, will provide axial strains expected to be produced under DBE level ground motions. The collapse level axial strains can be estimated by amplifying the demands for the DBE level. The required amplification is presented in Fig. 13 where for the 9 story BRBFs the ratios of the story drifts for collapse level to DBE level are plotted. The results show that the lateral drifts increase by 1.7 to 2.7 times when collapse level ground motions are considered as opposed to the DBE ground motions.

The modification to the deflection amplification factor eliminates the need to amplify the story drift by 2 times in order to estimate the inelastic response of the system. A more rational distribution of C_d helps the estimation of the interstory drifts at DBE level events. The recommendations of AISC341 can be modified to estimate the brace axial strains under collapse level ground motions. A conservative upper bound of 3.0 can be considered as that ratio of lateral drifts according to Fig. 13. This upper bound provides conservative estimates for the upper stories. In short, it is recommended that the axial strains determined considering DBE ground motions be amplified by 3.0 to estimate the mean axial strains under collapse level ground motions. Based on the proposed modifications, the brace axial strains should be estimated as follows:

$$\varepsilon_{br} = 3 \times \frac{C_d \times \theta_s}{\alpha} \times \sin\theta \times \cos\theta \tag{7}$$

7. Evaluation of the proposed modifications

The 24 archetype models were reconsidered in order to evaluate the acceptability of the proposed modifications. In the light of the C_d profile given in Eq. (6), all archetypes were redesigned. The proposed C_d profile

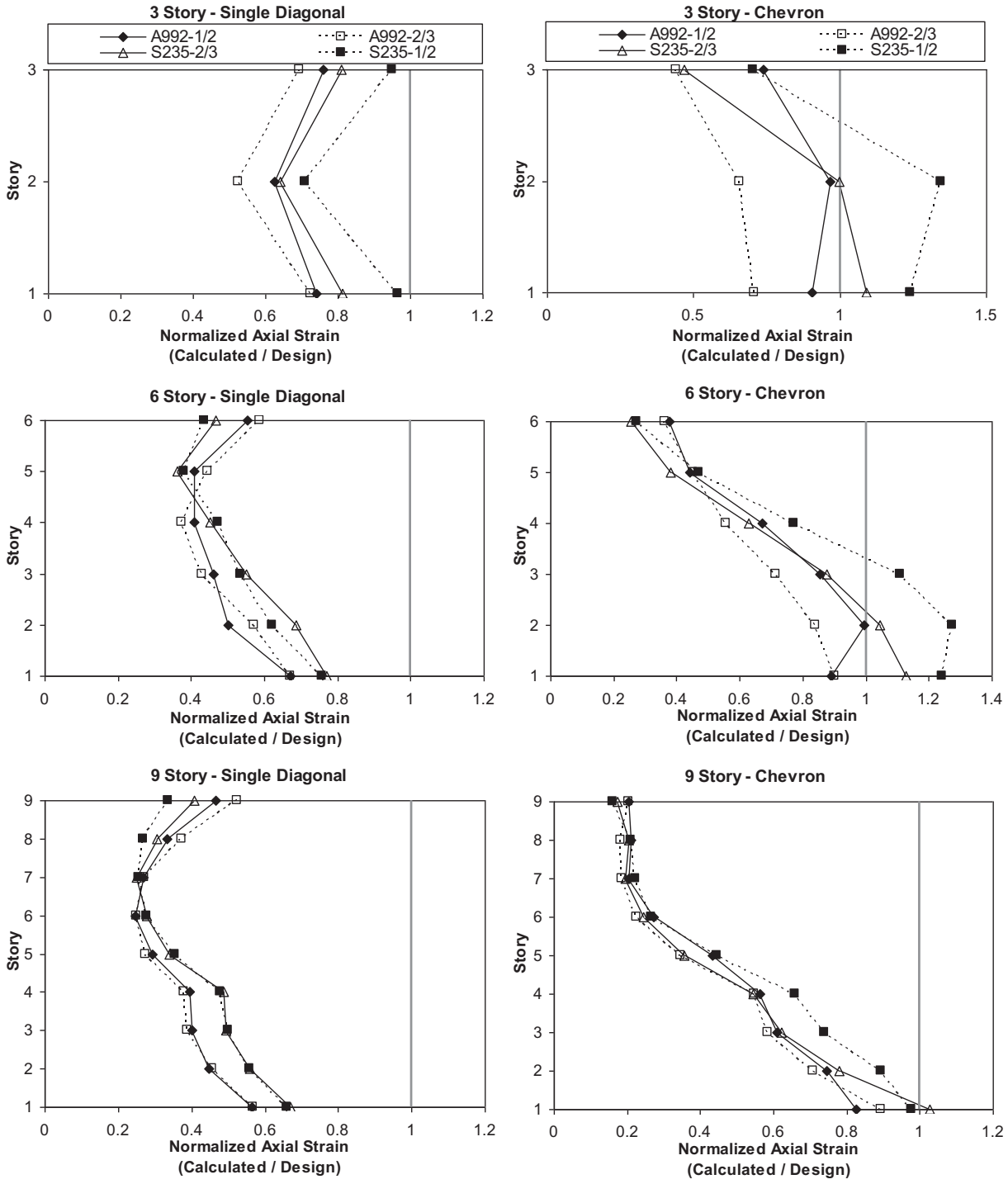

Fig. 14. Normalized brace axial strain for redesigned archetypes.

resulted in changes in member sizes for the single diagonal BRBFs, whereas no changes in member sizes were required for the chevron BRBFs. Because most of the single diagonal BRBF designs were governed by drift limitations, an increase in the C_d factor for the lower stories required brace member sizes to be updated for these systems. The redesigned brace sizes are indicated in Table 2. Note that the column and beam sizes remained the same after the redesign process. For the chevron type BRBFs, the original designs were governed by strength limit states, and increasing the C_d value for the lower stories did not result in a change in the member sizes, and hence the same member sizes were adopted.

Although the member sizes did not change for some of the frames, the design interstory drift and design brace axial strain values were updated according to a change in the C_d profile and an increase in the amplification for brace strains from 2.0 to 3.0. The updated values are indicated in Tables 3 through 6. The increased value of C_d at the lower stories and the increase in the amount of strain amplification resulted in higher brace axial strain demands, although the brace size remained the same. These would enable a much more accurate determination of the demands, such that the BRB member can be manufactured to accommodate these higher demands. The revised designs required a new set of inelastic

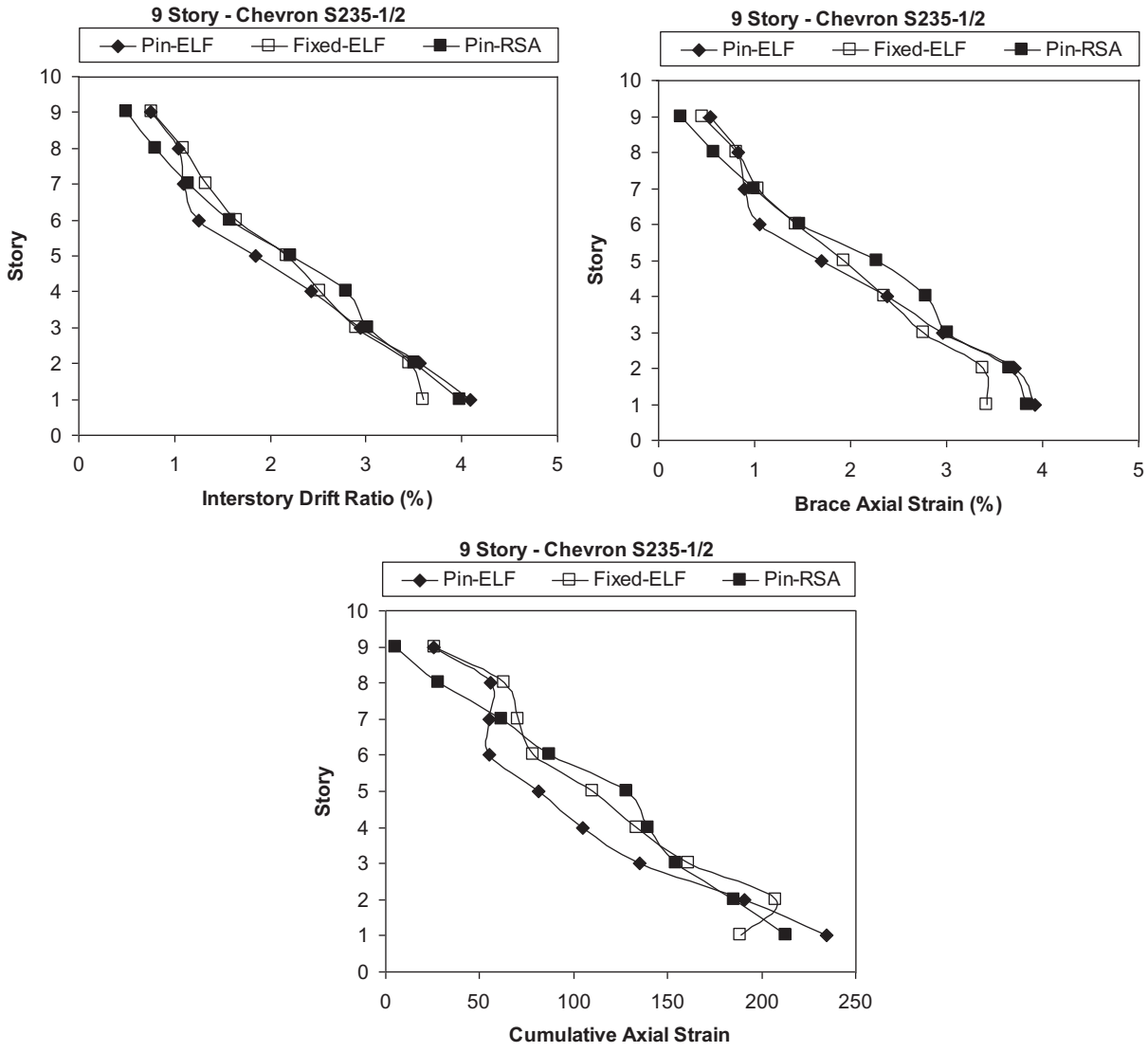

Fig. 15. Responses of BFBF archetypes designed and analyzed under various assumptions.

time history analyses to be conducted for evaluation purposes. This new set, however, only included the single diagonal archetypes because the brace members of these frames were changed. The interstory drift ratios and brace axial strains from these new set of analyses are not reported in tabular format but normalized values of the brace axial strain are presented in Fig. 14. According to this figure, the proposed modifications significantly enhance the estimated axial strains. The brace axial strain ratios stayed below unity indicating that the proposed modifications are adequate. There are cases in which the ratios exceed unity. These are particular to cases with the chevron type of bracing having 235 MPa of yield strength. The differences become more pronounced as the yielding length of the BRB gets shorter.

It should be emphasized that the proposed modifications do not result in significant changes in member sizes. In some cases, such as the chevron bracing archetypes, the proposed modification had an impact on the response quantities estimated at the design stage without having any impact on the member sizes. Therefore, the proposed modifications are not expected to significantly increase the weight and cost of a BRBF. On the other hand, for BRBF systems that are governed by drift limitations, adopting a single valued C_d such as 8.0 would negatively affect the cost of the framing, due to the difficulty associated with meeting the drift limits at the upper stories.

8. Limitations of the study and future research needs

The archetypes considered in this study were modeled to have pinned beam-to-column connections and pinned column bases. These assumptions were adopted so as to consider the worst case scenario, where the moment resistances of the beams and columns are not considered. In addition, the study was limited to the archetypes that were designed based on the ELF procedure. In certain taller (e.g., 12-, and 16-story) configurations, the use of the ELF procedure was found to result in a design that was overly conservative during beta testing of the methodology [15]. In these cases, the RSA procedure was used to avoid a conservative bias in the results. The archetypes designed based on the ELF and RSA procedures are expected to be similar, because the maximum story number was limited to 9 in the present study.

A limited number of analyses were conducted to investigate the impact of the assumptions used in this study. For this purpose the 9 story Chevron archetype with S235 core plates having a yielding length equal to 1/2 of the total length was considered. This archetype was redesigned using the RSA procedure and the member sizes are reported in Table 1. Comparing the member sizes of the two frames, it may be concluded that both the ELF and RSA procedures result in identical column sizes and similar brace sizes. Two additional frames were analyzed under collapse level ground motions. One of these frames is the one that employ

pinned connections but was designed according to the RSA procedure. The second one employs moment-resisting beam-to-column connections and fixed column bases, and this was designed according to the ELF procedure. The responses of the 3 frames are compared in Fig. 15 where interstory drift, brace axial strain and cumulative brace axial strain are reported. The results show that the two frames designed based on ELF or RSA procedures provide very similar responses. The use of moment resisting connections and fixed column bases has a greater impact on the results. While the general trends are similar, the interstory drift and brace axial strain are reduced in the first story, due to the fixity provided in the column bases. The reduction in response quantities is about 10% for the first story.

Future research should consider taller frames designed using the RSA procedure to extend the findings of this study. Different bracing configurations also need attention. Beta testing of the Methodology outlines possible performance groups to be considered for a complete assessment of the response factors used for BRBFs.

9. Conclusions

A numerical study on seismic response factors for BRBFs has been presented. Twenty-four BRBF archetypes were designed according to the U.S. provisions using the current values of response factors recommended in ASCE 7. The FEMA P695 methodology was adopted for the evaluation process. Interstory drift ratio, brace axial strain and cumulative brace axial strain were used as performance metrics. The results showed that most of the frames performed satisfactorily when interstory drift and cumulative axial strains were considered. In general, the interstory drifts stayed below 5%, and the cumulative axial strains stayed below 200 times the yield strain, where these values can easily be accommodated by BRBFs. On the other hand, marked differences between the design axial strain and the axial strain demand for collapse level ground motions were reported. For most of the archetypes the axial strain demand was more than 2 times the axial strain capacity of the BRB. The differences are attributed to the underestimation of interstory drifts at the design stage and the differences between the demands produced by collapse level and DBE ground motions.

A complementary study was conducted to investigate the deflection amplification for BRBFs. The results revealed that the amplification of deflections is non-uniform over the height of the building. The inelastic drifts were found to accumulate in the lower stories and the value of the deflection amplification factor (C_d) exceeded the current value of 5.0, which is recommended in the ASCE 7 standard. A C_d profile that varies over the height of the building was proposed which enables cost optimized solutions when compared with the use of a single valued deflection amplification factor.

The differences between the story drift demands produced due to collapse level and DBE ground motions were studied using time history analysis. The results showed that the story drifts amplify the DBE level by 1.7 to 2.7 times when collapse level ground motions are considered. A modification to the AISC 341 requirements for expected brace deformations was proposed which requires amplifying the DBE level demands by 3 times.

The proposed modifications to the C_d factor were applied to the archetype frames, which resulted in changes in member sizes for single diagonal type BRBFs but no change in member sizes for the chevron type BRBFs. The same performance metrics were considered for the redesigned frames and the results indicate that the proposed modifications to the deflection amplification factor and expected brace deformations provide acceptable solutions. The brace axial strains obtained at the design stage and the demands from collapse level ground motions are comparable. This would ensure proper design and manufacture of the BRBs to accommodate the brace axial strain demands.

References

[1] Q. Xie, State of the art of buckling-restrained braces in Asia, J. Constr. Steel Res. 61 (2005) 727–748.
[2] C. Uang, M. Nakashima, Steel buckling-restrained braced frames, Earthquake Engineering from Engineering Seismology to Performance Based Engineering, CRC Press, 2004.
[3] American Institute of Steel Construction (AISC), Seismic Provisions for Structural Steel Buildings. AISC, 2016 341–416.
[4] C.M. Uang, Establishing R (or Rw) and Cd factors for building seismic provisions, ASCE J. Struct. Eng. 117 (1) (1991) 19–28.
[5] American Society of Civil Engineers and Structural Engineering Institute (ASCE/SEI), Minimum Design Loads for Buildings and Other Structures, American Society of Civil Engineers, Reston, VA, 2016.
[6] D.R. Sahoo, S.H. Chao, Stiffness-based design for mitigation of residual displacements of buckling-restrained braced frames, ASCE J. Struct. Eng. 141 (2015) 1–13.
[7] S. Kiggins, C.M. Uang, Reducing residual drift of buckling-restrained braced frames as a dual system, Eng. Struct. 28 (2006) 1525–1532.
[8] A.F. Ghowsi, D.R. Sahoo, Seismic performance of buckling-restrained braced frames with varying beam-column connections, Int. J. Steel Struct. 13 (4) (2013) 607–621.
[9] N. Hoveidae, R. Tremblay, B. Rafezy, A. Davaran, Numerical investigation of seismic behavior of short-core all-steel buckling restrained braces, J. Constr. Steel Res. 114 (2015) 89–99.
[10] R. Sabelli, S. Mahin, C. Chang, Seismic demands on steel braced frame buildings with buckling restrained braces, Eng. Struct. 25 (2003) 655–666.
[11] L.A. Fahnestock, R. Sause, J.M. Ricles, Seismic response and performance of buckling-restrained braced frames, ASCE J. Struct. Eng. 133 (9) (2007) 1195–1204.
[12] M. Iwata, T. Kato, A. Wada, Performance evaluation of buckling-restrained braces in damage-controlled structures, in: F. Mazzolani (Ed.), Behavior of Steel Structures in Seismic Areas, Proc., 4th Int. Conf. STESSA 2003, Naples, Italy 2003, pp. 37–43.
[13] R.L. Mayes, C. Goings, N. Wassim, S. Harris, J. Lovejoy, J.P. Fanucci, P. Bystricky, J.R. Hayes, Comparative performance of buckling-restrained braces and moment frames, Proc., 13th World Conf. On Earthquake Engineering, Vancouver, B.C., Canada, 2004.
[14] Federal Emergency Management Agency (FEMA), Quantification of Building Seismic Performance Factors FEMA P695 ATC-63 Project Report, Federal Emergency Management Agency, Washington, DC, 2009.
[15] NEHRP Consultants Joint Venture, Evaluation of the FEMA P-695 Methodology for Quantification of Building Seismic Performance Factors, National Institute of Standards and Technology, US Department of Commerce, Engineering Laboratory, Gaithersburg, MD, 2010.
[16] M.S. Speicher, J.L. Harris, Collapse Prevention seismic performance assessment of new buckling restrained braced frames using ASCE 41, Eng. Struct. 164 (2018) 274–289.
[17] American Society of Civil Engineers and Structural Engineering Institute (ASCE/SEI). Seismic Rehabilitation of Existing Buildings. Reston, VA: American Society of Civil Engineers; 2013.
[18] W.A. Lopez, R. Sabelli, Seismic Design of Buckling-Restrained Braced Frames. Structural Steel Education Council, Steel Tips, 2004.
[19] American Institute of Steel Construction (AISC), Specification for Structural Steel Buildings, AISC, Chicago, IL, 2016.
[20] R. Tremblay, P. Bolduc, R. Neville, R. Devall, Seismic testing and performance of buckling-restrained bracing systems, Can. J. Civ. Eng. 33 (2006) 183–198.
[21] M. Bosco, E.M. Marino, P.P. Rossi, Design of steel frames equipped with BRBs in the framework of Eurocode 8, J. Constr. Steel Res. 113 (2015) 43–57.
[22] OPENSEES, Version 2.0 User Command-Language Manual, 2009.
[23] M.B. Bozkurt, C. Topkaya, Development of welded overlap core steel encased buckling-restrained braces, J. Constr. Steel Res. 127 (2016) 151–164.
[24] A. Zona, A. Dall'Asta, Elastoplastic model for steel buckling-restrained braces, J. Constr. Steel Res. 68 (2012) 118–125.
[25] J. Newell, C.M. Uang, Cyclic behavior of steel wide-flange columns subjected to large drift, ASCE J. Struct. Eng. 134 (8) (2008) 1334–1342.
[26] G. Ozkula, J. Harris, C.M. Uang, Observations from cyclic tests on deep, wide-flange beam-columns, AISC Eng. J. (2017) 45–59.
[27] S. Merritt, C.M. Uang, G. Benzoni, Subassemblage Testing of Star Seismic Buckling Restrained Braces, Department of Structural Engineering, University of California, San Diego, La Jolla, California, 2003.
[28] M. Dehghani, R. Tremblay, Design and full-scale experimental evaluation of a seismically endurant steel buckling-restrained brace system, Earthq. Eng. Struct. Dyn. 47 (2018) 105–129.
[29] L.J. Jia, H. Ge, R. Maruyama, K. Shinohara, Development of a novel high-performance all-steel fish-bone shaped buckling-restrained brace, Eng. Struct. 138 (2017) 105–119.
[30] N.M. Newmark, W.J. Hall, Earthquake Spectra and Design, Earthquake Engineering Research Institute, El Cerrito, Calif, 1982.
[31] C.M. Uang, A. Maarouf, Deflection amplification factor for seismic design provisions, J. Struct. Eng. 120 (8) (1994) 2423–2436.
[32] A. Kuşyılmaz, C. Topkaya, Displacement amplification factors for steel eccentrically braced frames, Earthq. Eng. Struct. Dyn. 44 (2) (2015) 167–184.
[33] A. Kuşyılmaz, C. Topkaya, Evaluation of seismic response factors for eccentrically braced frames using FEMA P695 Methodology, Earthquake Spectra 32 (1) (2016) 303–321.